Published by Institute of Physics Publishing for SISSA/ISAS
Received: *November 10, 2004*
Accepted: *December 22, 2004*

# D-Sitter space: causal structure, thermodynamics, and entropy

**Michal Fabinger and Eva Silverstein**

*SLAC and Department of Physics, Stanford University*
*Stanford, CA 94305/94309, U.S.A.*
*E-mail:* fabinger@ias.edu, evas@slac.stanford.edu

Abstract: We study the entropy of concrete de Sitter flux compactifications and deformations of them containing D-brane domain walls. We determine the relevant causal and thermodynamic properties of these "D-Sitter" deformations of de Sitter spacetimes. We find a string scale correspondence point at which the entropy localized on the D-branes (and measured by probes sent from an observer in the middle of the bubble) scales the same with large flux quantum numbers as the entropy of the original de Sitter space, and at which Bousso's bound is saturated by the D-brane degrees of freedom (up to order one coefficients) for an infinite range of times. From the geometry of a static patch of D-Sitter space and from basic relations in flux compactifications, we find support for the possibility of a low energy open string description of the static patch of de Sitter space.

Keywords: D-branes, Superstring Vacua, AdS-CFT and dS-CFT Correspondence.



 http://jhep.sissa.it/archive/papers/jhep122004061/jhep122004061.pdf

## Contents



## 1. Introduction and summary

Flux compactifications play a very important role in string theory. They provide examples of backgrounds with fixed moduli, both in potentially realistic settings with small internal compact spaces [1]–[7] and in canonical examples of the AdS/CFT correspondence where the compact space is a large Einstein space [8]. In both these cases, a negative contribution to the effective moduli potential (coming from positive scalar curvature, orientifold planes, or 7-branes wrapped nontrivially on 4-cycles in the base of elliptically fibred Calabi-Yau fourfold compactifications of F theory [2]) plays off against positive contributions (including energy contained in quantized fluxes) to produce a local minimum. In a natural class of models where we scale up the RR flux quantum numbers $Q_{RR}$ leaving other parameters fixed, the string coupling is fixed at a value of order

$$g_s \sim \frac{1}{Q_{RR}}\,. \tag{1.1}$$

In this paper, we will study the entropy of flux compactifications, focusing on the de Sitter case, via a simple relation of de Sitter flux compactifications to deformations of them which we will refer to as "D-Sitter" spaces. These are spacetimes containing D-brane domain walls surrounding a bubble of a different de Sitter vacuum.

We will analyze explicitly basic properties of D-Sitter and corresponding de Sitter flux compactifications, and apply this analysis to obtain two basic results.

One of the main results will be a comparison of the entropy carried locally on the D-branes, probed by an observer in the middle of the bubble, with that of the original de Sitter space. This will lead to an interesting string scale "correspondence point" at which they agree up to order one factors, somewhat similar to the black hole correspondence point studied in [9, 10].

The other main result will be circumstantial evidence pointing toward a low energy open string theory in the de Sitter causal patch, with of order $Q_{RR}$ ways for the open strings to end on the horizon. This evidence will be twofold. First, we will exhibit a set of observers whose causal patch has a static coordinate system for which one can take a limit in which the D-branes of the D-Sitter space approach the horizon as the D-Sitter space approaches the original de Sitter space. Second, we will show that a cutoff of order string scale on $Q_{RR}^2$ D-brane worldvolume field theory degrees of freedom, combined with the basic flux stabilization result (1.1), produces an entropy agreeing with the de Sitter entropy. An open string picture of horizons has been advocated in [11], and we interpret our results as providing some concrete but circumstantial evidence for this picture, and an avenue toward studying it explicitly to which we hope to return in future work.[1] Of course an open string theory on the causal patch of the perturbative de Sitter solution does not account for decays of de Sitter models [1, 5, 14] (which avoid some of the puzzles raised in e.g. [15, 16, 17]); we leave for future work the description of these decays from the D-Sitter point of view.

Having listed the main results, let us now turn to a more extensive summary of the motivation and the elements of our analysis.

In AdS/CFT examples, the physics of the flux compactification is equivalent to that of a large-$N$ dual field theory. This provides a holographic description of the background. In particular, the logarithm of the total number of states of the cutoff field theory (which we will refer to as the Susskind-Witten entropy) can be compared to that contained in AdS, and in the simplest case of $\mathcal{N} = 4$ super-Yang-Mills one finds an entropy scaling like $N^2$ on both sides [18].

The relatively well understood AdS/CFT examples arise from near horizon limits of brane systems, while generic flux compactifications based on Calabi Yau or orbifold internal spaces, even those that reduce to AdS as opposed to dS or Minkowski space, have not been constructed from such a near horizon limit. Also the simplest AdS/CFT examples have a tunable dilaton, while generically this modulus is fixed (or runs away) in flux compactifications.

[1] Recent examples of other time dependent backgrounds usefully described in terms of open strings have been proposed in [12, 13] and many related works.



JHEP12(2004)061

However, one can still study the entropy $S(\{Q_i\})$ associated with a generic flux background as a function of the flux quantum numbers $\{Q_i\}$. Moreover, one can trade fluxes for branes in a region of the gravity background by introducing a bubble whose wall is made up of D-branes.

In AdS/CFT examples, this procedure produces the gravity dual of the field theory on its Higgs or Coulomb branch, for which BPS states can be followed adiabatically. We can implement this procedure much more widely, applying it to dS flux compactifications where we do not know a field theory dual.

In the AdS/CFT case, this procedure could be applied step by step, pulling a small number of D-branes out of the horizon in each step. Then calculating the spectrum of strings stretched to the horizon from the branes would provide a microscopic accounting of the derivative of the Susskind-Witten entropy with respect to flux quantum numbers. It is not yet known how to do this calculation of the stretched string spectrum. One can however pull of order $N$ branes out of the horizon in the gravity dual of a large-$N$ field theory (as in the simplest example of [19]) and thus transform of order $N^2$ of the entropy into states localized on the D-branes.

In this paper, we will evaluate the entropy carried by D-brane bubbles obtained by deformation from dS and AdS flux compactifications, and compare it to the entropy associated to the flux compactifications themselves.

To begin, we will analyze the thermodynamic and causal properties of the de Sitter spacetimes containing bubbles (which we will refer to as D-Sitter spacetimes), which turns out to be quite interesting in its own right. In particular, a priori one might think that there is no equilibrium thermodynamic ensemble in which to compute the entropy because the branes separate phases of different dS cosmological constant (and thus naively they feel different temperature on the two sides of their worldvolume). However, as we will see here, by taking into account the acceleration of the brane observer on at least one side and the resulting Rindler temperature, one can identify a well-defined temperature on the D-branes and work consistently in a canonical thermodynamic ensemble.

We will determine the causal patches of important classes of observers in the D-Sitter spacetimes. One important type of observer has a static causal patch identical to that of ordinary de Sitter space, so that the deformation from de Sitter to D-Sitter changes only what is behind the horizon for this observer. The observer in the middle of the bubble will also play an important role. This observer's causal patch is not static but has very interesting properties: it contains the D-branes which carry entropy, and at the same time has a smaller horizon area at the moment of time symmetry than the original de Sitter causal patch so that as we increase the brane entropy we decrease the entropy associated with the horizon.

For generic D-Sitter spacetimes, we will find that in the canonical ensemble applying to our system, the entropy localized on the branes which is probed by this observer is much smaller than the original de Sitter entropy. Other excitations not localized on the D-branes, such as strings stretching from the D-branes to the horizon of this observers causal patch, are Boltzmann suppressed in the canonical ensemble but perhaps could play a role analogous to that of the states counted in the full Susskind-Witten entropy in the AdS case.

However, we will exhibit an interesting "correspondence point" related to that of [9, 10] at which the D-brane entropy approaches the dS entropy. In this correspondence limit, the Bousso bound [20] also approaches saturation for all positive global times.

Brane observers have a static coordinate system parameterizing their causal patch, as do observers maintaining a fixed distance from the branes. For these latter observers, one can take a limit in which the branes approach a trajectory tracking a portion of the observer horizon and in which the observer's causal patch approaches that of the original de Sitter space. This latter result may provide a concrete avenue toward realizing the goal of formulating horizon physics via open strings [11]. Closed strings exiting the horizon effectively have a boundary there, and the relation to D-branes we uncover in this paper may help in formulating this string theory as an open string theory. As we will see, the naive estimate that this putative open string theory has of order $Q_{RR}$ Chan-Paton indices and should be described as a field theory cut off at the string scale gives the correct entropy for de Sitter space once we include the basic relation (1.1) coming from the flux stabilization of the dilaton in real models.

This paper is organized as follows. In section 2, we will explain the deformation between flux compactifications and D-brane bubbles, share a motivating analogy to our procedure in ordinary AdS/CFT, and briefly discuss the Susskind-Witten entropy of more general AdS flux vacua. In section 3, we turn to the de Sitter case. We explain the causal structure and thermodynamics of the DS (D-Sitter) spacetimes. In section 4, we discuss the thermal equilibrium of the domain walls. In section 5, we determine the entropy carried by the branes as observed by probes sent from an observer in the middle of the bubble, focusing on case of horizon sized bubbles, and explain the "correspondence point" at which this is comparable to the dS entropy. In section 6, we analyze Bousso's bound in D-Sitter spacetime. In section 7, we focus on the observers with a static causal patch and present our circumstantial evidence for an open string interpretation. In section 8 we conclude with a summary and some discussion of open questions.

Other approaches to the microscopic counting of dS entropy have appeared in [21]–[28]. Other works have recently studied nonperturbative decays of flux compactifications arising when brane bubbles dynamically nucleate [29, 30, 31, 14, 5] following [32, 33] and many other works; a recent discussion of thick wall decays occurs in [34]. In [35] appears an investigation of entropy associated with dS slices of dS space.

## 2. The basic deformation, and warmup AdS examples

One can rather generally obtain sets of D-branes associated to any flux background by deforming the system to one containing D-brane bubbles as in figure 1. The procedure is the following. Let us consider a compactification on $X$ down to $d$ dimensions. Given flux $\int_C F = Q_R$ on a cycle $C$ of the compactification, we can introduce $Q$ D-branes wrapped on a dual cycle $\tilde{C}$ sourcing the same RR field strength $F$. This set of D-branes is locally a domain wall in the $d$-dimensional spacetime, on one side of which (say the right side) the flux is $Q_R$ and on the left side of which the flux is $Q_L \equiv Q_R - Q$. For these different flux quantum numbers, the rest of the spacetime adjusts itself to solve the equations of

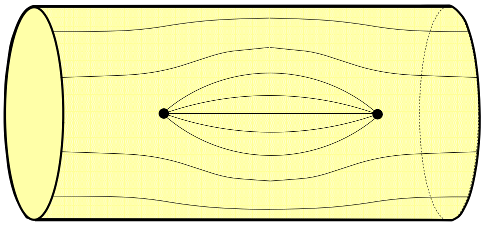

**Figure 1:** In a compactification of string theory with fluxes, we can locally change the amount flux through a certain cycle by introducing branes wrapped on the dual cycle.

motion on each side in the presence of the corresponding quantized flux. Topologically this is always possible, though generically this will lead to time dependent solutions, and in some cases the evolution will take the system out of theoretical control.

Our general strategy will be to consider cases where the resulting D-brane system is under control, and to study the entropy of the system both in the original flux compactification and in the D-brane bubble spacetime obtained from this deformation.

In black hole physics, one could deform a set of D-branes into a black hole by dialing the 't Hooft coupling $g_s Q$, and in appropriate cases count the entropy precisely using the D-brane worldvolume theory [36]. While our goal (transmuting the system into a system of D-branes whose states are easier to count) is similar, note that the deformation we are considering is different from that of [36]. In order to deform from the D-brane bubble spacetime into the original flux compactification, we must shrink the bubble (which generically requires going over a barrier). As we will discuss in the next subsection, this is analogous to moving on the moduli space of the field theory side of AdS/CFT rather than dialing the 't Hooft coupling.

This difference with the black hole case of [36], combined with the basic difference that there is no unbroken supersymmetry in our de Sitter case, will leave us with less conclusive results than [36]. Still, we will be able to obtain results similar to the D-brane cases of the black hole correspondence principle [9, 10], and we will obtain results from flux compactification which are nontrivially consistent with an open string interpretation of the de Sitter causal patch.

D-brane domain walls have been applied fruitfully for example in [37, 31, 38] to describe important aspects of the physics of gauge/gravity dual pairs, as well as to studying nonperturbative decays of flux compactifications arising when brane bubbles dynamically nucleate [29, 30, 31, 14, 5] following [32, 33]. Here, we will apply it to the question of the microscopic accounting of the entropies associated with flux compactifications. We will focus on the de Sitter case in later sections, but here we will begin with the very instructive case of AdS.

### 2.1 AdS/CFT analogy and motivation

In the usual AdS/CFT correspondence, one can deform the gravity side background smoothly into one in which there are D-branes separating an AdS region from say flat space [19]. In the holographic dual field theory, this is a deformation corresponding to

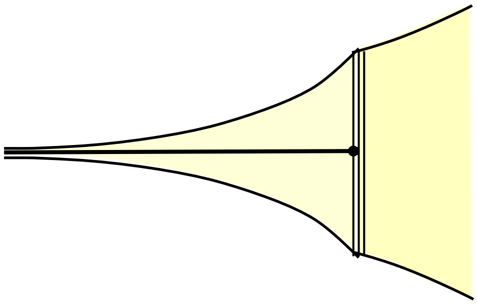

**Figure 2:** Anti D-Sitter space: a D-brane domain wall consisting of $Q$ D3-branes separates a region of flux $N_R$ to the right of the wall from a region of flux $N_L = N_R - Q$ to the left of the wall. For $Q \ll N_R$, the difference in entropy at low energies goes like $2QN_L$, the number of strings stretched from the branes to the horizon. It is not known how to calculate this number directly on the gravity side of AdS/CFT. For $Q$ of order $N_R$, on can count states localized on the D-branes to obtain an entropy of the same order in flux quantum numbers as the original anti de Sitter space.

going out on the Coulomb branch of the U($N$) $\mathcal{N} = 4$ super Yang-Mills theory. If we consider the entropy corresponding to simply a count of the total number of states in the Hilbert space below some cutoff [18], then we can adiabatically follow the states as we move onto the Coulomb branch. In particular, for BPS states we expect of order $N^2$ massive off-diagonal BPS "W boson" states to be identifiable after the deformation, and this corresponds to the fact that the bubble wall of D-branes in the [19] model carries entropy of order $N^2$ from off diagonal stretched strings. Thus in this case, the BPS states are still visible on the gravity side, but have become massive stretched string states.[2] In other words, if we had not known about the full AdS/CFT duality obtained by taking a near horizon limit, but instead just had the $AdS \times S$ flux compactification itself, we could still have obtained by this method a nontrivial microscopic rendering of the BPS Susskind-Witten entropy of the system in terms of degrees of freedom on D-branes.

One can also study a Coulomb branch configuration corresponding to taking $Q \ll N_R$ branes out of an original stack of $N_R$ branes and separating them from $N_L = N_R - Q$ remaining branes. This corresponds in the near horizon region to a domain wall containing $N$ D3-branes separating a phase of flux $N_R$ from one of flux $N_L \equiv N_R - Q$. The change in the number of degrees of freedom as we pull the $Q$ branes away is of order $QN_L$ and comes mostly from strings stretching from the domain wall to the horizon of the Poincare patch. If we could independently count these strings purely on the gravity side, then this would provide a microscopic accounting of the derivative of the entropy with respect to the flux quantum number. It is not known how to do this counting; in any case in a fixed temperature ensemble these strings are Boltzmann suppressed. As we have seen, in the AdS case we can simply trade all of the flux for branes in the flat region of the [19] examples.

In our de Sitter case, we will also not be able to count such stretched strings and will instead focus on the question of how many states are localized on the D-brane wall

[2] In this example, the non-BPS states are as always more difficult to follow, and there appears to be substantial non-BPS entropy available in the flat region inside the spherical shell of [19]; e.g. one could put a Schwarzschild black hole there.



JHEP12(2004)061

itself. These strings alone will be able to saturate the dS entropy in a string scale "correspondence point". It would be very interesting to develop techniques to count the strings stretched to the horizon in both the AdS and dS cases. We will leave this for future work.

An interesting variant on this case is to carry out the same procedure for situations with fractional branes, i.e. orbifolds of AdS/CFT [39] such as $AdS_5 \times S^5/Z_k$. Then although the flux integrated over the cycle $S^5/Z_k$ is $N$, the total entropy is $kN^2$ rather than $N^2$ as our naive estimate would indicate. In this case, one could deduce this from the D-brane domain wall configuration in the near horizon limit by the presence of $k$ sectors of wound strings.

AdS vacua having no known interpretation as near horizon limits of branes arise from flux compactifications as discussed recently in various approaches [1, 7]. In the KKLT models yielding AdS vacua (i.e. before the introduction of the anti D3-brane which uplifts the AdS to dS in their construction), the Susskind-Witten entropy as a function of flux quantum numbers can be estimated. As we will show in section 5.4, the Bousso-Polchinski mechanism allows one to tune the cosmological constant very finely, leading to an entropy that can be as large as of order

$$S \sim Q^{\frac{\chi}{2}+4} \tag{2.1}$$

in terms of a flux quantum number $Q$ where $\chi$ is the Euler characteristic of the Calabi-Yau fourfold compactification of F theory. The result (2.1) is much larger than the naive entropy on D-branes of order $Q^2$. However, it is intriguing in its dependence on the integer flux quantum numbers, perhaps suggesting a dual gauge theory with many flavors. It is conceivable that this indicates a phenomenon like that of fractional branes just reviewed.

## 3. Causal structure and Penrose diagrams

Let us now move on to our main interest of de Sitter flux vacua. We will be interested in the entropy carried by the D-branes in the D-Sitter spacetimes which are deformations of de Sitter space with D-brane bubbles. In ordinary de Sitter space, each observer determines a causal patch, and the horizon of area $A$ in this causal patch has been argued to carry an entropy accessible to this observer $A/4l_d^{d-2}$ in terms of the $d$-dimensional Planck scale $l_d$ [40]. As we discussed in section 1, we can deform dS to DS by introducing D-brane bubbles. In this section we will begin our analysis of these spacetimes by determining their causal structure, including an explicit specification of the Penrose diagrams for D-Sitter. This will enable us to determine the causal patches for various observers which replace the causal patch of the original de Sitter space for those observers. For an important class of D-Sitter solutions, there is at least one observer whose causal patch remains the same as in the original de Sitter space. For an observer in the middle of the bubble, the causal patch has a smaller horizon area than the original de Sitter causal patch, and in the case of a bubble of flat space the size of the original dS horizon this area shrinks to zero. For observers maintaining a fixed distance from the branes, there is a static coordinate system covering their causal patches. This causal patch has the interesting property that one can take a limit in which the D-branes approach the horizon for these observers.



JHEP12(2004)061

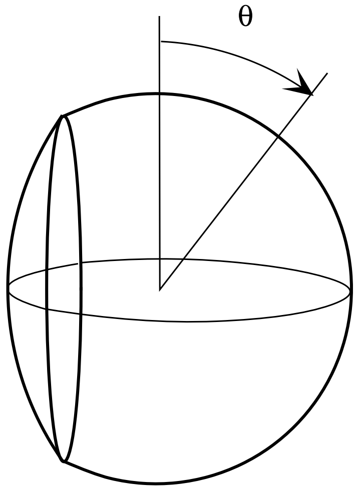


**Figure 3:** This figure shows a solution of the euclidean Einstein's equations, with two regions of different cosmological constants ($\Lambda_L < \Lambda_R$) separated by a massive brane. In the thin wall approximation, matching the metrics on two sides of the brane is done using the Israel junction conditions. By Wick-rotating the $\theta$ coordinate one obtains a solution of lorentzian Einstein's equations which contains two different de Sitter vacua connected to each other by a brane. We refer to such lorentzian solutions as 'D-Sitter'.

### 3.1 Penrose diagrams

Let us now analyze the causal structure of the D-Sitter spacetimes which arise as analytic continuations of the euclidean solutions from figure 3 to lorentzian signature. These spacetimes contain a spherical domain wall which first contracts, and then expands again. The domain wall separates two regions (referred to as $dS_L$ and $dS_R$) of different cosmological constants ($\Lambda_L$ and $\Lambda_R$). Our strategy will be to analytically continue $\theta$ in each of those regions separately. We will work mainly in the thin wall approximation, and comment on the thick wall generalization at the end.

Let us consider one particular side of the euclidean solution. The round sphere metric is given by

$$ds^2 = d\theta^2 + \sin^2\theta \; d\Omega_{d-1}^2 \, . \tag{3.1}$$

After the analytic continuation $\theta \to i\tau + \pi/2$, this becomes de Sitter space in global coordinates

$$ds^2 = -d\tau^2 + \cosh^2\tau \, d\Omega_{d-1}^2 \, . \tag{3.2}$$

It is convenient to define a new time coordinate — the conformal time $T$

$$\frac{1}{\cos T} = \cosh\tau \, , \qquad T \in \left(-\frac{\pi}{2}, \frac{\pi}{2}\right) , \tag{3.3}$$

and to expand $d\Omega_{d-1}^2$ as

$$ds^2 = \frac{1}{\cos^2 T}(-dT^2 + d\theta'^2 + \sin^2\theta' \, d\Omega_{d-2}^2) \, . \tag{3.4}$$

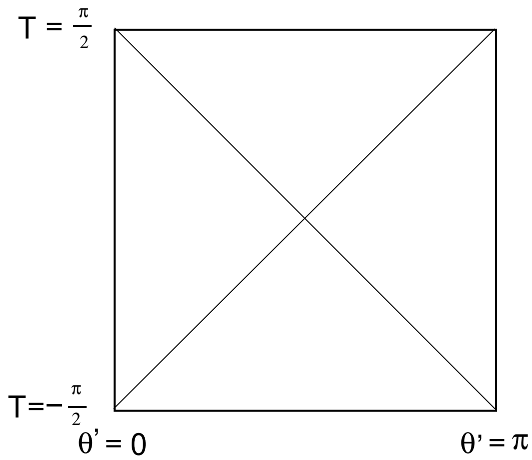


**Figure 4:** Penrose diagram of de Sitter space. Over each point in this picture there is an $S^{d-2}$, which degenerates to a zero size at $\theta' = 0$ and $\theta' = \pi$. Every horizontal slice is an $S^{d-1}$. The diagonal lines represent light rays originating from the poles of the $S^{d-1}$ at $T = -\pi/2$.



Now, suppressing the $S^{d-2}$ directions, we obtain the Penrose diagram in figure 4. Only a part of it will be relevant for us at this point.

In a full global de Sitter, the range of the coordinate $\theta'$ would be $(0, \pi)$. In the D-Sitter spacetimes it will be restricted to

$$\theta'_L \in (0,\, \theta'_{LB}(T_L))\,, \qquad \theta'_R \in (\theta'_{RB}(T_R),\, \pi) \tag{3.5}$$

on the left and on the right, respectively, because of the presence of the domain wall. We would like to find the precise form of the time-dependence of the position of the domain wall (or the 'bubble'). In other words, we want to identify the functions $\theta'_{LB}(T_L)$ and $\theta'_{RB}(T_R)$.

This can be easily done using the original euclidean solution. Its embedding $(d+1)$-dimensional flat space may be expressed as

$$\begin{aligned} x_1 &= R\cos\theta \\ x_2 &= R\sin\theta\cos\theta' \\ x_\alpha &= R\sin\theta\sin\theta' n_\alpha\,, \quad \alpha = 3\ldots(d+1)\,, \end{aligned} \tag{3.6}$$

where $\sum_\alpha n_\alpha^2 = 1$. The coordinates $x_i$ satisfy

$$x_1^2 + x_2^2 + \sum_{\alpha=3}^{d+1} x_\alpha^2 = R^2\,. \tag{3.7}$$

The worldvolume of the domain wall is the intersection of (3.7) with

$$x_2 = \pm\sqrt{R^2 - R_B^2}\,, \tag{3.8}$$

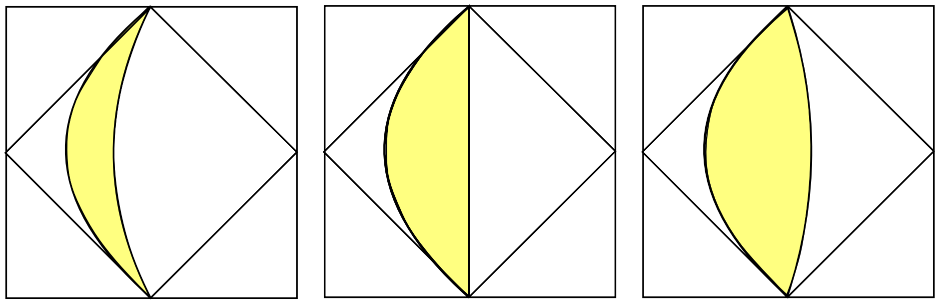


**Figure 5:** D-Sitter spacetimes with a $(a)$ 'subcritical' bubble, $\theta'_{RB}(T_R) < \pi/2$, $(b)$ 'critical' bubble, $\theta'_{RB}(T_R) = \pi/2$, and $(c)$ 'supercritical' bubble $\theta'_{RB}(T_R) > \pi/2$. In all cases we choose $\Lambda_L < \Lambda_R$, which means $R_L > R_R$. The shaded regions are absent from the spacetimes. In each case the two boundary lines of the shaded regions are to be identified.

where only one sign on the right hand side should be considered. From (3.6) and (3.8) we obtain

$$\cos\theta' = \pm\sqrt{1 - \frac{R_B^2}{R^2}}\,\frac{1}{\sin\theta}\,. \tag{3.9}$$

After the analytic continuation $\theta \to i\tau + \pi/2$ this becomes (using (3.3))

$$\cos\theta' = \pm\sqrt{1 - \frac{R_B^2}{R^2}}\,\cos T\,. \tag{3.10}$$

Thus we have obtained the explicit time-dependence of the position of the domain wall

$$\cos\theta'_{LB}(T_L) = \pm\sqrt{1 - \frac{R_B^2}{R_L^2}}\,\cos T_L\,, \tag{3.11}$$

$$\cos\theta'_{RB}(T_R) = \pm\sqrt{1 - \frac{R_B^2}{R_R^2}}\,\cos T_R\,. \tag{3.12}$$

All combinations of signs are possible here except having a minus sign in (3.11) and a plus sign in (3.12). We will always choose $R_L > R_R$.

The corresponding Penrose diagrams are depicted in figure 5.

Having determined the position of the domain wall for each side in terms of $T_L$ and $T_R$ respectively, we can now match the two solutions by determining how the left and right coordinates on the bubble should be identified. That is, we would like to know which time $T_L$ at the domain wall corresponds to which $T_R$ at the same point. Again, this can be easily found using the original euclidean solution where (cf. (3.6))

$$R_L\cos\theta_L = R_R\cos\theta_R\,. \tag{3.13}$$

After the analytic continuation we obtain

$$R_L\,\sinh\,\tau_L = R_R\,\sinh\,\tau_R\,. \tag{3.14}$$

Expressed in terms of time $T_L$ and $T_R$ at the bubble this is

$$\frac{1}{\cos^2 T_L} = 1 + \frac{R_R^2}{R_L^2}\left(\frac{1}{\cos^2 T_R} - 1\right). \tag{3.15}$$

These relations are general (given the thin wall approximation). It is useful to distinguish three types of bubbles depending on whether the bubble is at the horizon size at $\tau = 0$, below the horizon size, or above. Let us take for simplicity the case that $\Lambda_L \ll \Lambda_R$. (As we will review in section 5, it is possible in flux models to discretely tune $\Lambda$ to be very close to zero [30, 5, 1].) This means that the bubble is superhorizon size from the point of view of the $dS_L$. From the point of view of the $dS_R$, the bubble can be subhorizon sized, horizon sized, or superhorizon sized. As reviewed in [5], these cases correspond to a brane tension $T_B$ whose square is less than, equal to, or greater than a critical value $T_c^2 = 2(d-2)(d-1)^{-1}(\Lambda_R - \Lambda_L)l_d^{4-2d}$ [33]. We will refer to these bubbles as subcritical, critical, and supercritical, respectively.

The Penrose diagrams we have determined so far (figure 5) had two separate pieces, each corresponding to one side of the domain wall, along with a prescription for identifying the points on the bubble wall to join the two pieces together. This might be sufficient for our purposes since we know how to map the points of the domain wall from one part of the Penrose diagram to the other. However, it may still be interesting to see how to construct one global (and connected) Penrose diagram from the two parts. In order to do so, we will have to perform a (conformal) coordinate transformation at least on one side.

Our strategy will be the following. We want to find a global coordinate system $(\theta'_G, T_G)$ such that in the left part of the spacetime $(\theta'_G, T_G)$ are functions of $(\theta'_L, T_L)$, and in the right part of the spacetime $(\theta'_G, T_G) = (\theta'_R, T_R)$. We require that also in the new $(\theta'_G, T_G)$ coordinate system the light-cones are at 45 degrees. This means, of course, that the transformation from $(\theta'_L, T_L)$ to $(\theta'_G, T_G)$ must be conformal, i.e. of the form

$$T_G + \theta'_G = f(T_L + \theta'_L)\,, \qquad T_G - \theta'_G = g(T_L - \theta'_L)\,, \tag{3.16}$$

where $f$ and $g$ are some functions. We have to make sure that at the domain wall the coordinates match correctly onto the right part of the Penrose diagram, where we decided to keep the original coordinates (i.e. where we chose $(\theta'_G, T_G) = (\theta'_R, T_R)$). This requirement translates into

$$T_R + \theta'_{RB}(T_R) = f(T_L + \theta'_{LB}(T_L))\,, \tag{3.17}$$

and

$$T_R - \theta'_{RB}(T_R) = g(T_L - \theta'_{LB}(T_L))\,, \tag{3.18}$$

where the functions $\theta'_{LB}(T_L)$ and $\theta'_{RB}(T_R)$ are given by (3.11) and (3.12), and where the times $T_L$ and $T_R$ are related by (3.15). The conditions (3.17) and (3.18) determine the explicit form of the functions $f$ and $g$ in the conformal transformation (3.16).

The resulting connected Penrose diagrams are in figure 6.

So far we have considered the idealized case where the domain wall is infinitely thin. One can also construct Penrose diagrams for spacetimes where the domain wall has a finite thickness. The causal structure is nevertheless very similar to the idealized case. (This



JHEP12(2004)061

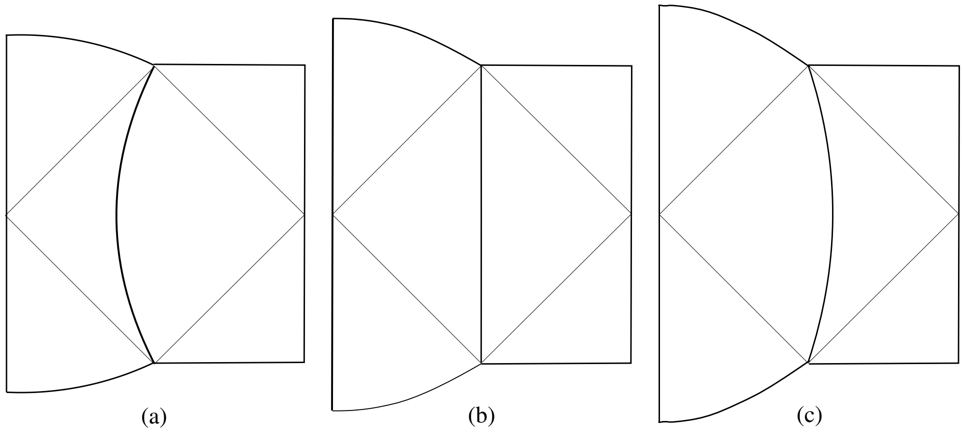


**Figure 6:** Another rendering of the Penrose diagrams of D-Sitter spacetimes with a $(a)$ 'subcritical' bubble, $\theta'_{RB}(T_R) < \pi/2$, $(b)$ 'critical' bubble, $\theta'_{RB}(T_R) = \pi/2$, and $(c)$ 'supercritical' bubble $\theta'_{RB}(T_R) > \pi/2$. In all cases we choose $\Lambda_L < \Lambda_R$, which means $R_L > R_R$.

case has been analyzed recently in [34] following [32] in the context of bubble nucleation.) The analytic continuation of the euclidean solution for a thick wall would suggest an exponentially growing wall thickness in the lorentzian continuation. However, as long as the force holding the brane together is stronger then that coming from the de Sitter expansion, in the stable lorentzian solution the brane's thickness will not grow exponentially and its intersection with future infinity in the Penrose diagram will be just a point.

## 3.2 Causal patches in D-Sitter

We now turn to the question of the causal patches for observers in the D-Sitter spacetimes. In the Penrose diagram for ordinary de Sitter space (figure 4) each point represents an $S^{d-2}$, which shrinks to zero size at the left and right edges of the diagram. These edges are natural geodesics on which to place observers (both in $dS$ and $DS$) which we will refer to as "left" and "right" observers $\mathcal{O}_L$ and $\mathcal{O}_R$ respectively. In $dS$, each of these observers determines a causal patch, the triangles on the left and right sides of the figure. The static patch coordinates

$$ds^2 = -\left(1 - \frac{r^2}{R_{dS}^2}\right) dt^2 + \frac{dr^2}{1 - \frac{r^2}{R_{dS}^2}} + r^2 d\Omega_{d-2}^2 \qquad (3.19)$$

reveal a horizon at $r = R_{dS}$. The time coordinate $t$ in the static patch goes to $\pm\infty$ at the two interior edges of the triangle (at $T = \pm(\theta' - \pi/2)$), and goes through zero at the central vertex of the triangle (at $T = 0, \theta' = \pi/2$). At $t = 0$, $r = 1$ the transverse $S^{d-2}$ has area $A \sim R_{dS}^{d-2}$. Here sit the states accounting for the de Sitter entropy according to the "hot tin can" picture developed e.g. in [15] (which we will briefly review in section 6).

We would like to know what the analogous results are for the D-Sitter spacetime. In the D-Sitter spacetime, there are several interesting classes of observers.

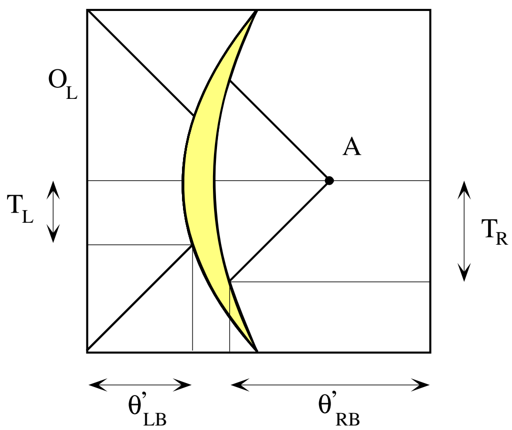


**Figure 7:** Calculation of the horizon area of the observer $\mathcal{O}_L$ sitting on the left of the Penrose diagram, i.e. at $\theta' = 0$.

**Left observer's causal patch.** Let us first focus on the observer $\mathcal{O}_L$ in the center of the bubble in the $dS_L$ part of the space. For subcritical bubbles and critical bubbles, the right observer $\mathcal{O}_R$ has the same causal patch as in ordinary $dS_R$.

In particular, we would like to compute the geometry of the causal patch and the horizon area of $\mathcal{O}_L$ (see figure 7).

First, we need to find the time $T_L$ when the light ray $\mathcal{L}_1$ reaches the domain wall,

$$\theta'_{LB}(T_L) = T_L + \frac{\pi}{2}\,. \tag{3.20}$$

Using (3.11) we can rewrite (3.20) as

$$\frac{1}{\cos^2 T_L} = \left(2 - \frac{R_B^2}{R_L^2}\right). \tag{3.21}$$

This value of $T_L$ translates via (3.15) into the following $T_R$,

$$\frac{1}{\cos^2 T_R} = \frac{R_L^2 + R_R^2 - R_B^2}{R_R^2}\,, \tag{3.22}$$

and from (3.12) we see that the corresponding $\theta'_{RB}$ satisfies

$$\sin^2\theta'_{RB} = \frac{R_L^2}{R_L^2 + R_R^2 - R_B^2}\,. \tag{3.23}$$

A short examination of figure 7 reveals that the horizon are of the left observer at $T = 0$ is given by

$$A = |\Omega_{d-2}| R_R^{d-2} \sin^{d-2}(\theta'_{RB} + T_R)\,, \tag{3.24}$$

where $T_R$ and $\theta'_{RB}$ are given by (3.22) and (3.23), and where $|\Omega_{d-2}|$ stands for the volume of a unit $S^{d-2}$.

Notice that for $R_L \gg R_R$, $sin^2\theta'_{RB} \to 1$ so $\theta'_{RB} \to \pi/2$ while $cos^2 T_R \to 0$ so $T_R \to -\pi/2$. This means $A \to 0$. In general, the horizon area we have calculated satisfies $A < A_R$, so adding branes (which carry some entropy) goes along with a decrease in the horizon area. We will exhibit an explicit relation expressing this tradeoff in section 5.1.

We can simplify this result to obtain

$$A = |\Omega_{d-2}| R_R^{d-2} \left( \frac{R_L R_R + \sqrt{(R_R^2 - R_B^2)(R_L^2 - R_B^2)}}{R_L^2 + R_R^2 - R_B^2} \right)^{d-2} . \tag{3.25}$$

For critical bubbles, $R_R = R_B$ and $A = |\Omega_{d-2}| R_R^{d-2} (R_R/R_L)^{d-2}$.

Note that the causal patch we have derived for the left observer $\mathcal{O}_L$ is not a *static* patch: the proper area of the bubble wall grows in time and so one cannot find static coordinates describing the whole left causal patch containing the bubble. The horizon area also changes as a function of time in the left causal patch. Both the D-brane entropy and the entropy associated with the horizon area grow in time for $\tau > 0$.

There is a set of observers whose causal patch is also static; these are the brane observers and those at a fixed distance from them, to which we turn next.

**Static patches in D-Sitter.** In ordinary de Sitter space, one can identify a certain part of the space — referred to as the 'static patch' — in which there exists a time-like Killing vector field. One can find many distinct static patches in a given global de Sitter space (cf. figures 11 and 12). All of them are however equivalent up to the action of the de Sitter group $\mathrm{SO}(d-1,1)$. Each static patch turns out to be the causal patch of some observer ( i.e. it is the set of points which are in both the causal past of at least one point of the observer's worldline, and in the causal future of some other point of the observer's worldline).

We would like to find the static patches in D-Sitter spacetimes.[3] Of course, in the case of the subcritical bubble (figure 5$a$), the causal patch of the right observer will be static, and it will not contain the bubble at all. Depending on the precise shape of the bubble, this will also be true for other observers with $\theta'$ not too far from $\pi$. There can be, however, more static patches in the D-Sitter space.

The static patch of the usual de Sitter space (and its natural coordinate system) can be obtained by an analytic continuation from the euclidean de Sitter solution, i.e. from a $d$-dimensional sphere. One writes the $S^d$ as an $S^1$ fibration over a hemisphere $S^{d-1}/\mathbb{Z}_2$ in such a way that there is a manifest U(1) isometry corresponding to motions along the $S^1$ fiber. The metric on the $S^{d-1}/\mathbb{Z}_2$ base is chosen to be independent of the fiber coordinate $\phi_d$. Then by Wick-rotating $\phi_d$ one obtains a patch of de Sitter space which is static. The static patch extends up to a horizon, located at the boundary of the $S^{d-1}/\mathbb{Z}_2$ (where in the euclidean solution the $S^1$ fiber was degenerate).

We will repeat this construction here. Eventually, we will restrict our coordinates to range only up to the place where we want to place the domain wall. In this way we will obtain one side of a static patch in D-Sitter.

[3]We would like to thank L. Susskind for a question leading us in this direction.

Let us choose the following coordinates for the $S^d$.

$$\begin{aligned}
y_1 &= R\cos\phi_1 \\
y_2 &= R\sin\phi_1\cos\phi_2 \\
y_3 &= R\sin\phi_1\sin\phi_2\cos\phi_3 \\
&\vdots \\
y_d &= R\sin\phi_1\sin\phi_2\sin\phi_3\cdots\cos\phi_d \\
y_{d+1} &= R\sin\phi_1\sin\phi_2\sin\phi_3\cdots\sin\phi_d\,.
\end{aligned} \tag{3.26}$$

The $\phi_1,\ldots,\phi_{d-1}$ parameterize the $S^{d-1}/\mathbb{Z}_2$ base, and the $\phi_d$ is the $S^1$ fiber coordinate. The range of $\phi_i$ for $i<d$ is $[0,\pi)$, and the range of $\phi_d$ is $[0,2\pi)$. The metric of the $S^d$ can be written as

$$\frac{ds^2}{R^2} = d\phi_1^2 + \sin^2\phi_1\,d\phi_2^2 + \sin^2\phi_1\sin^2\phi_2\,d\phi_3^2 + \cdots + \sin^2\phi_1\sin^2\phi_2\sin^2\phi_3\cdots\sin^2\phi_{d-1}\,d\phi_d^2\,. \tag{3.27}$$

By the Wick rotation $\phi_d \to i\tilde{t}$, we get the metric of the de Sitter static patch

$$\frac{ds^2}{R^2} = d\phi_1^2 + \sin^2\phi_1\,d\phi_2^2 + \sin^2\phi_1\sin^2\phi_2\,d\phi_3^2 + \cdots - \sin^2\phi_1\sin^2\phi_2\sin^2\phi_3\cdots\sin^2\phi_{d-1}\,d\tilde{t}^2\,. \tag{3.28}$$

Now we will consider the spatial geometry at some definite $t=\text{const}$. The horizon will be located at

$$\sin^2\phi_1\sin^2\phi_2\sin^2\phi_3\ldots\sin^2\phi_{d-1} = 0\,. \tag{3.29}$$

Even though this condition looks complicated, it is actually equivalent to

$$\sin\phi_{d-1} = 0\,, \tag{3.30}$$

because if $\sin\phi_i = 0$ for any $i < d-1$, the $\phi_{d-1}$ coordinate becomes degenerate, and we may as well say that $\sin\phi_{d-1} = 0$. Given the fact that we chose $\phi_{d-1}$ to be in $[0,\pi)$, we can rewrite (3.30) as

$$\phi_{d-1} = 0\,. \tag{3.31}$$

In terms of the embedding coordinates of the $S^{d-1}/\mathbb{Z}_2$

$$\begin{aligned}
\tilde{y}_1 &= R\cos\phi_1 \\
\tilde{y}_2 &= R\sin\phi_1\cos\phi_2 \\
\tilde{y}_3 &= R\sin\phi_1\sin\phi_2\cos\phi_3 \\
&\vdots \\
\tilde{y}_{d-1} &= R\sin\phi_1\sin\phi_2\sin\phi_3\cdots\cos\phi_{d-1} \\
\tilde{y}_d &= R\sin\phi_1\sin\phi_2\sin\phi_3\cdots\sin\phi_{d-1}
\end{aligned} \tag{3.32}$$

(which have to satisfy $\tilde{x}_d \geq 0$) the condition (3.31) is simply

$$\tilde{y}_d = 0\,. \tag{3.33}$$

For $d-1=2$ we could say that the horizon (i.e. the $\tilde{y}_d = 0$ curve) is well approximated by the union of the Greenwich meridian and the international date line (see figure 8). For an observer living in the US, the world is terminated there, and the eastern hemisphere does not exist. In higher dimensions, the $\tilde{y}_d = 0$ curve becomes an $S^{d-2}$ surface dividing the $S^{d-1}$ into two halves. Only one half has a physical significance.

For the reader's convenience, we will also provide an explicit coordinate redefinition which transforms the metric in the de Sitter static patch (3.28) into the most standard form. Notice that using (3.32) we can rewrite (3.28) as

$$ds^2 = -\tilde{y}_d^2\, d\tilde{t}^2 + \sum_{i=1}^{d} d\tilde{y}_i^2\,, \qquad \sum_{i=1}^{d} \tilde{y}_i^2 = R^2\,, \tag{3.34}$$

with the indicated constraint imposed on the $\tilde{y}_i$ coordinates. It is easy to check that with the following definitions

$$t = R\tilde{t}\,, \qquad r^2 = R^2 - \tilde{y}_d^2\,, \qquad \Omega_i = \frac{\tilde{y}_i}{\sqrt{R^2 - \tilde{y}_d^2}}\,, \qquad i = 1, \dots (d-1)\,, \tag{3.35}$$

the static patch metric (3.28) becomes

$$ds^2 = -\left(1 - \frac{r^2}{R^2}\right) dt^2 + \frac{dr^2}{1 - r^2/R^2} + r^2 d\Omega^2\,. \tag{3.36}$$

Now we can ask where we can place the domain wall inside the static patch. In the euclidean solution, the brane could have been at the intersection of the sphere (3.26) with any plane

$$a_1 y_1 + a_2 y_2 + \cdots + a_d y_d + a_{d+1} y_{d+1} = \text{const.}\,, \tag{3.37}$$

such that the radius of the spherical cut is $R_B$. However, we have Wick-rotated $\phi_d$. Because the definition of $y_d$ and $y_{d+1}$ contains $\phi_d$, we must set $a_d = a_{d+1} = 0$ in (3.37). Otherwise, the brane would not be static in the 'static patch'. Thus we can express the position of the brane purely in terms of the $\tilde{y}_i$ ($i < d$) coordinates defined in (3.32),

$$a_1 \tilde{y}_1 + a_2 \tilde{y}_2 + \cdots + a_{d-1} \tilde{y}_{d-1} = \text{const.} \tag{3.38}$$

We can also use an SO$(d-1)$ coordinate redefinition to transform (3.38) into

$$\tilde{y}_{d-1} = \text{const.} \tag{3.39}$$

Notice that viewed from the embedding space, the brane is 'perpendicular' to the horizon: the brane is at $\tilde{y}_{d-1} = $ const., whereas the horizon is at $\tilde{y}_d = 0$. In other words, the brane is at a line (or surface) of a constant latitude, whereas the horizon has a fixed longitude, namely $\phi_{d-1} = 0^o$ or $\phi_{d-1} = 180^o$. The resulting situation is depicted in figure 8, and a schematic picture of this spatial slice is depicted in figure 9.

We have determined how the static patch looks on one side of the domain wall. Of course, on the other side the situation will be qualitatively the same, so the only task remaining is to find how these static patches fit into the global geometry of the D-Sitter space.

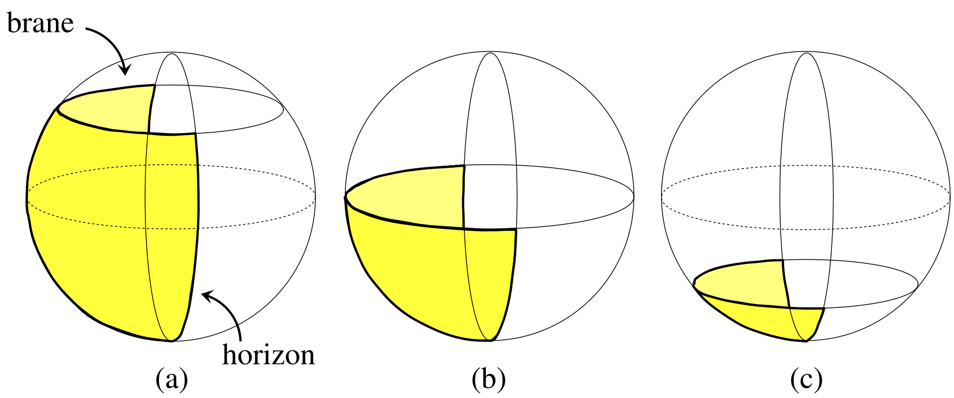


**Figure 8:** The shaded surfaces in this figure represent the spatial geometry on one side of the brane in the static patch at some definite $t =$ const. To obtain the full spatial geometry of the static patch, one needs to glue together two surfaces of this type. The different cases in this figure are chosen to match the three possibilities for the right part of the diagrams in figures 5 and 6.

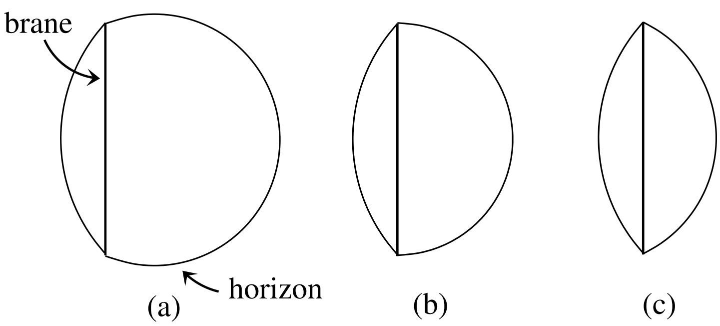


**Figure 9:** A schematic picture of the spatial geometry of the static patch at $t =$ const. On each side of the brane the spatial curvature of the horizon is different. The branes are not really straight, as can be seen from figure 8. Note that as the tension of the branes decreases (moving from right to left in the sequence depicted here), they approach a part of the horizon and the static patch approaches that of de Sitter space ($dS_R$).

This question is however very easy to answer. Any observer staying inside one particular static patch never looses causal contact with the brane. For this reason in the asymptotic past and the asymptotic future the observer's worldline must come to the same point in the Penrose diagram (see figure 10) as some part of the brane itself. (This does not mean that the observer must actually touch the brane, a sufficient condition is to stay a finite distance from the brane at all times.) The whole static patch can be therefore interpreted as the causal patch of some definite observer. (Of course, the causal patch cannot be larger than the static patch because it is impossible to return from behind the horizon.) The embedding of the static patch into the global D-Sitter is depicted in figure 10.

For completeness, we include also figures of the static patches two dimensional de Sitter and D-Sitter. We should remember, however, that this case is rather special because $S^0$ is not a manifold, but simply just two points.



JHEP12(2004)061

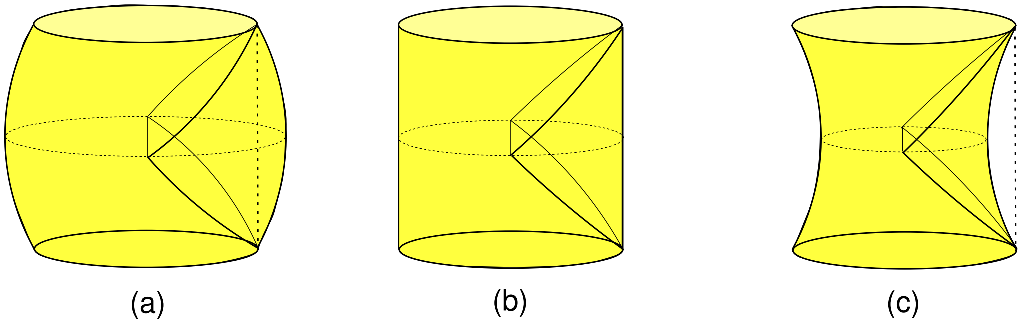


**Figure 10:** Embedding of the static patch into the global geometry of D-Sitter space. Each 'cylinder' represents a region of a definite cosmological constant in D-Sitter space, and its boundary is the location of the brane. The static patch is the causal patch of the observer whose worldline is indicated by the dotted line. The full global geometry of the D-Sitter (with a full static patch embedded in it) corresponds to two diagrams of this type, one for each side of the brane.

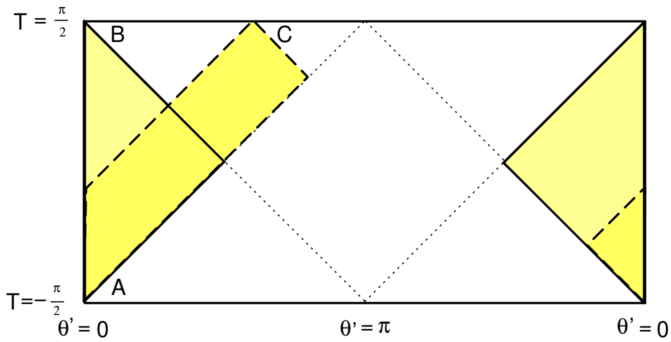


**Figure 11:** The Penrose diagram of de Sitter space for $d = 2$. Note that this Baby Sitter has rather special properties since $S^0 = \mathbb{Z}_2$. The two vertical edges of the diagram should be identified because the spatial slice of the global geometry is a circle. The picture shows one static patch, which is the causal patch of an observer originating in $A$ and arriving at $B$, and another static patch, which is the causal patch of someone starting at $A$ and going to $C$. All the static patches are equivalent up to actions of the SO$(1,1)$ de Sitter group.

In the next section, we will study the thermodynamic properties of the brane worldvolume theory.

## 4. Thermal equilibrium of the domain walls

We will be interested in the thermodynamics of our domain walls separating two regions of different cosmological constants. One of the first questions that arises is whether they are in thermal equilibrium. Naively, one might expect that this would not be the case because the domain walls are separating regions of different de Sitter temperatures. We will see, however, that there is a subtle interplay between the de Sitter expansion and the acceleration of the branes leading to a well-defined temperature which is constant in time.

Let us first consider the most simple case in which the cosmological constant in the left part of the spacetime vanishes, and the bubble is critical (figure 5$b$), $R_B = R_R$. We



JHEP12(2004)061

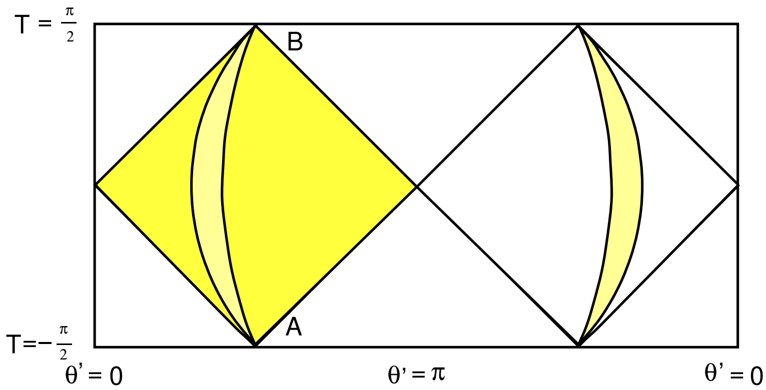


**Figure 12:** The shaded square in this figure shows a nontrivial static patch in a two-dimensional D-Sitter space. There are also trivial static patches, the causal patches of observers living close to $\theta' = \pi$, which do not contain the brane at all.

would like to know what will be the response of a particle detector located at a fixed position on the expanding (or shrinking) domain-wall. From the point of view of the right part of the spacetime, the detector is following a geodesic in de Sitter space, and it will see a constant temperature given by the de Sitter radius $\mathcal{T} = 1/2\pi R_R$. From the point of view of the left part of the spacetime (which is flat), the worldline of the detector is no longer a geodesic. Instead, it is a hyperbola corresponding to a constant proper acceleration $a = 1/R_B = 1/R_R$. For this reason, the detector should register a constant Rindler temperature given by $\mathcal{T} = a/2\pi = 1/2\pi R_R$. We see that the two temperatures agree, and the detector can be in a thermal equilibrium at the temperature $\mathcal{T} = 1/2\pi R_R$.

Similarly, the observer $\mathcal{O}_L$ in the middle of the brane (figure 7) observes a thermal bath similar to that arising from the moving mirror problem as long as the reflection coefficient at the transition between the two cosmological constants is nonzero. We will analyze the constraints required to avoid back reaction from this effect in flux compactifications in section 5.5.[4]

A very simple result can be obtained also for general D-Sitter spacetimes. One way to argue for this is to consider the euclidean version of the geometry.[5] The euclidean analog of the detector trajectory is a circle of radius $R_B$, and for each detector there is a U(1) isometry of the solution which generates motions along this circle. For this reason the propagator $G(\Delta s)$ between two points on the circle separated by a distance $\Delta s$ along the circle will have a singularity for every $\Delta s = 2\pi n R_B$, $n \in \mathbb{Z}$. Translated into the lorentzian geometry this means that the propagator $G(\Delta\tau)$ between two points on the detector trajectory (separated by a proper time interval $\Delta\tau$) will have singularities for imaginary $\Delta\tau$ whenever $\Delta\tau = 2\pi i n R_B$, $n \in \mathbb{Z}$. It can be shown that the presence of these

[4]Thanks to S. Hellerman and S. Shenker for discussions on this point.

[5]We will consider only the lorentzian vacuum whose Green's functions can be obtained by an analytic continuation of the euclidean Green's functions.

singularities implies that the detector will register a thermal radiation at temperature

$$\mathcal{T} = \frac{1}{2\pi R_B} \,. \tag{4.1}$$

(For more details, see for example the discussion related to equations (3.58) and (3.67) of [41].) Because in this derivation we did not need to specify whether we think about the detector as being on the left or on the right side of the domain wall, it is clear that the detector can be in thermal equilibrium. The corresponding equilibrium temperature is given by (4.1).

This temperature (4.1) is what the brane observer measures locally. In general, the effective temperature in general relativity depends on position and on the observer making the measurement due to blueshifting effects arising from nontrivial warping by $g_{00}$. As we discussed in the previous section, the brane observer in the full geometry has a static patch with effective temperature diverging at the horizon, leading to an entropy that depends on position on the branes which is dominated by the region near the horizon and is as difficult to calculate as that of the original de Sitter static patch due to cutoff dependence.

However, other observers such as the left observer $\mathcal{O}_L$ (figure 7) can probe entire spatial slices of the D-brane worldvolume by sending out probes in all directions toward the bubble wall. Suppose the left observer $\mathcal{O}_L$ sends a spherically symmetric probe to the branes which will reach the branes around the time $\tau = 0$. Then because the branes do not coincide with the horizon for the left observer, $g_{00} \sim 1$ there, and $\mathcal{O}_L$ observes the brane degrees of freedom at the local brane temperature (4.1) and carrying the corresponding extensive brane worldvolume entropy to a good approximation. In the next section, we will calculate this entropy in our D-Sitter spacetimes.

## 5. D-brane entropy as probed by observer $\mathcal{O}_L$ in critical D-Sitter

Given the well-defined thermodynamics we have developed in the previous section, we can now study the entropy carried by the D-branes in the D-Sitter spacetimes obtained from flux compactifications. We have in mind the models [1, 5] whose relevant properties we will collect here and in section 5.2. As we will see, the input from the models is relatively simple and will apply rather generally. In this section, we will focus on the entropy accessible to probes sent by the observer $\mathcal{O}_L$ in the middle of the bubble. (In section 7, we will discuss the open string physics of the static observer $\mathcal{O}_s$.)

For simplicity we will here consider critical bubbles with flux quantum numbers (i.e. D-brane charges) $\vec{Q}$ separating a phase of $\Lambda_R \sim 1/R_R^2$ with flux quanta $\vec{Q}_R$ from a phase of smaller cosmological constant $\Lambda_L \sim 1/R_L^2$ with flux quanta $\vec{Q}_L = \vec{Q}_R + \vec{Q}$ such that $\Lambda_R - \Lambda_L$ is of order $\Lambda_R$. This includes the possibility of $\Lambda_L$ tuned to approximately zero.

Here we are organizing the quantized RR fluxes into a vector $\vec{Q}_\gamma$ (where $\gamma$ refers to the flux vacuum of interest, so that e.g. $\gamma = R(L)$ refers to the right (left) de Sitter vacuum respectively in the D-Sitter spacetimes introduced in section 2). The kinetic term for the RR fields, $\int F \wedge *F$ then determines the leading $\vec{Q}_\gamma$-dependence of the potential energy in a given flux model

$$\vec{Q}_\gamma^2 \equiv Q_\gamma^2 \equiv \int (F \wedge *F)_\gamma \,. \tag{5.1}$$

We will assume that the moduli other than the dilaton are stabilized near order one, putting in some order 1 fudge factors to represent their effects, and we will focus on the dilaton dependence. So on a torus or toroidal orbifold model [5, 4, 3] one would obtain simply $\vec{Q}_\gamma^2 \sim \sum_i q_i Q_i^2$ with $q_i$ of order 1, but on a general Calabi-Yau the structure will be more complicated. In our application we will be interested in the gross scaling of various quantities with the magnitudes $Q_\gamma$.

Clearly there are many interesting ways to deviate from and refine these choices, but we will see that these specifications are sufficient to answer the most basic questions we are interested in regarding the entropy comparisons. In the following, the symbol $\sim$ will refer to relations that hold up to coefficients that are of order one, by which we mean coefficients which do not go to zero or infinity as we scale up the RR flux quantum numbers.

### 5.1 Model independent analysis

Let us begin by determining the entropy without inputting any information about the flux stabilization of the dilaton in the concrete models. Then in the next subsection we will add the constraints from the flux stabilization mechanism. A horizon sized bubble has a tension $T_H$ satisfying [33]

$$T_c^2 = \frac{2(d-2)(\Lambda_R - \Lambda_L)}{(d-1)l_d^{2d-4}} \tag{5.2}$$

where $l_d$ is the $d$-dimensional Planck length. Given our specification that $\Lambda_R - \Lambda_L \sim \mathcal{O}(\Lambda_R)$, we can simplify (5.2) to $T_c^2 \sim \Lambda_R / l_d^{2d-4}$.

The tension of the $D-(d-2)$-branes which form the bubble wall is[6]

$$T_D = \frac{\alpha Q}{g_s l_s^{d-1}} \sim \frac{\alpha Q g_s^{\frac{d}{d-2}}}{l_d^{d-1}} \tag{5.3}$$

where $\alpha$ is a fudge factor meant to indicate the order one parameters that affect the D-brane tension;[7] in the second form we have used the relation $g_s^2 l_s^{d-2} \sim l_d^{d-2}$.

Plugging (5.3) into (5.2) leads to the following relations.

$$\frac{R_R}{l_s} \sim \frac{1}{\alpha g_s Q} \,. \tag{5.4}$$

The entropy $S_R$ associated with the $dS_R$ horizon is given by

$$S_R \sim \frac{R_R^{d-2}}{l_d^{d-2}} \sim \frac{Q^2}{\alpha^{d-2}(g_s Q)^d} \,. \tag{5.5}$$

[6]Here the $d-2$ refers to the spatial Neumann directions of the D-branes in the de Sitter dimensions; the branes wrap cycles in the internal space whose dependence we are suppressing here.

[7]In the supercritical MSS models [5], it happens that $\alpha$ is significantly smaller than one for models with a cosmological constant tuned to be much smaller than string scale, so for such cases we will have in mind the KKLT models [1].



JHEP12(2004)061

We are interested in understanding the entropy carried on the D-branes. The $(d-1)$-dimensional D-brane field theory has an effective 't Hooft coupling constant which runs with energy scale; evaluating it at the scale of the temperature $\mathcal{T}_{\mathcal{R}} \sim 1/R_R$ we found for critical bubbles in section 4 gives (using also (5.4))

$$g_{\text{eff}}^2 \sim \frac{Qg_{YM}^2}{\mathcal{T}_R^{5-d}} = \frac{Qg_s}{(\mathcal{T}_R l_s)^{5-d}} \sim \alpha^{d-5}(Qg_s)^{d-4}\,. \tag{5.6}$$

In order to proceed, we need to understand the range of couplings of interest to us. From (5.4), we see that if we confine ourselves to the region

$$\frac{R_R}{l_s} \geq 1 \tag{5.7}$$

then we have

$$\alpha g_s Q \leq 1\,. \tag{5.8}$$

For $d>4$, this means (from (5.6)) that the effective 't Hooft coupling $g_{\text{eff}}$ is $\leq 1/\sqrt{\alpha}$, and we can apply perturbative field theory.

For $d=4$, the effective 't Hooft coupling satisfies $g_{\text{eff}} \sim 1$, so we have to look more closely to determine whether we can reliably study the physics of the D-brane. The effective Yang-Mills coupling itself (as opposed to the 't Hooft coupling) satisfies

$$\frac{(g_{YM}^{(d=4)})^2}{\mathcal{T}_R} \sim \frac{1}{Q} \ll 1 \tag{5.9}$$

using (5.4).

We believe this is enough to give control, as is suggested by the work on nonconformal versions of AdS/CFT [42]. For $d=4$ our D-brane is effectively a $D2$-brane (if we suppress the compact dimensions), for which the Yang-Mills coupling runs to zero in the UV and becomes strong in the IR. The $D2$-brane solution has three distinct regions as one moves radially (corresponding to the worldvolume RG flow). Near the boundary, the solution is highly curved corresponding to the UV free Yang-Mills theory. At $g_{\text{eff}}$ of order 1, it transitions to a weakly curved region accessible to supergravity analysis. For the ordinary $D2$-brane of type-IIA theory, it is not until the effective Yang-Mills coupling $g_{YM}^2/energy$ itself becomes very large that the solution crosses over to the M2-brane solution. We see from (5.9) that since we are interested in $Q \geq 1$ (mostly $Q \gg 1$ in fact), $g_{YM}^2/\text{energy} \ll 1$ and we should expect results similar to those in the two $D2$-brane regions.

Of course our D-branes are not literally type-IIA D2-branes. Microscopically, they are IIB D5-branes wrapped on three-cycles of a compactification manifold in the critical geometric KKLT models of [1], and noncritical D-branes of various dimensions wrapped on cycles of the asymmetric orientifold in the MSS models [5]. They are codimension one objects in the de Sitter directions. In general, we expect to have distinct $\alpha'$ and $g_s$ expansions, which for D-brane solutions are controlled by the effective 't Hooft coupling $g_{\text{eff}}$ and $(g_sQ)/Q$ respectively. The large $Q$ expansion is good when the dilaton $g_s$ is sufficiently weak even if $\alpha'$ effects are nontrivial. This is true for $g_{\text{eff}} \sim 1$ if $Q$ is large, which is our situation (5.9).

In this regime, in the large $Q$ limit the entropy on the D-branes is of the form

$$S_D = f(g_{\text{eff}})Q^2 R_B^{d-2}\mathcal{T}_B^{d-2} \tag{5.10}$$

where $\mathcal{T}_B \sim 1/R_B$ is the D-brane temperature (4.1). (Again, it is worth emphasizing that here we are discussing the extensive entropy on the D-branes accessible to measurements performed by the observer $\mathcal{O}_L$, who is in causal contact with all points on the branes and sees the extensive D-brane entropy (5.10).)

Using this relation, we can simplify (5.10) to

$$S_D = f(g_{\text{eff}})Q^2\,. \tag{5.11}$$

For future reference we also note here that from [42] the proper thickness of the brane solution is of order

$$L_{\text{branes}} \sim l_s g_{\text{eff}}^{\frac{1}{2}}\,. \tag{5.12}$$

(Of course this should not be taken literally for $g_{\text{eff}} < 1$ since GR will break down in this regime; in this regime we should expect an effective thickness of order $l_s$.)

From these relations, we see that if $f(g_{\text{eff}})$ is of order one, the D-brane entropy $S_D$ is

$$S_D \sim Q^2\,, \tag{5.13}$$

and its relation to the $dS_R$ entropy $S_R$ is

$$S_D \ll S_R \qquad \text{for } R_R \gg l_s \tag{5.14}$$

and

$$S_D \sim S_R \qquad \text{for } R_R \sim l_s\,. \tag{5.15}$$

This latter limit is obtained if

$$g_s \to \frac{1}{Q} \tag{5.16}$$

which in particular means that $g_{\text{eff}}$ approaches order one. In this same limit, the thickness of the brane solution (5.12) approaches $l_s$. $f(g_{\text{eff}})$ is of order 1 for $g_{\text{eff}} \sim 1$ in many D-brane systems studied, so we believe this is a reasonable assumption.

We will refer to this limit (5.15) as the "correspondence point", and will discuss in section 5.6 its relation to the usual correspondence point for black hole physics [9, 10].

In section 5.3 we will find that in the flux stabilization models the correspondence point is achievable and arises when $\Lambda_R$ is of order the maximum classically stable cosmological constant available in the models.

Applying the formula (3.25) for the area of the horizon in the left observer $\mathcal{O}_L$'s causal patch, in the case of a nearly flat bubble $R_L \gg R_R$, we can obtain a precise relation expressing the tradeoff in entropy observed by $\mathcal{O}_L$ between the horizon and the bubbles. Combining (3.25), (5.3), and (5.13), we obtain

$$\frac{R_L^2}{R_R^2}\left(\frac{A}{|\Omega_{d-2}|}\right)^{\frac{2}{d-2}} + R_B^2 R_R^2 \frac{\alpha^2 g_s^4}{l_4^2(d-2)^2} S_D = 2(2R_R^2 - R_B^2)\,. \tag{5.17}$$

This expresses a tradeoff between horizon entropy and brane entropy for $\mathcal{O}_L$ at $\tau = 0$.

### 5.2 Model input: generalities

In this subsection we will collect some of the relevant details from the flux stabilization models leading to $dS$ vacua. These models make use of contributions to the moduli potential-coming from fluxes (at order $g_s^0$ in string frame), orientifolds and other sources of negative tension arising at order $g_s^{-1}$ in string frame, and positive contributions to the potential coming at leading order $g_s^{-2}$ in string frame–to stabilize the dilaton. All the moduli are stabilized by this type of mechanism, by orbifolding, or by perturbative and nonperturbative quantum corrections to the $d$-dimensional effective potential.

Focusing on the dilaton dependence, the cosmological term to the first three orders in the $g_s$ expansion is of the form [5]

$$\Lambda_\gamma(g_s) = \frac{g_s^{\frac{4}{d-2}}}{l_d^2}\left(a - b_\gamma g_s + \frac{b_\gamma^2}{4a}(1+\delta_\gamma)g_s^2 + \mathcal{O}(g_s^3)\right) \tag{5.18}$$

where the subscript $\gamma$ refers to which $RR$ flux and brane configuration has been chosen. The third term comes from the kinetic terms $\int F_{RR}\wedge * F_{RR}$ for the RR field strengths $F_{RR}$, so

$$\frac{b_\gamma^2}{4a}(1+\delta_\gamma) \sim Q_\gamma^2\,. \tag{5.19}$$

The other two terms have the following origin in the microscopic models. For the KKLT models [1], $a \sim Q_{NSNS}^2$ since the $H_{NSNS}$ kinetic term arises at order $1/g_s^2$ in string frame; $b \sim \frac{\chi}{24} - N_3 - N_{\bar{3}}$ where $N_3, N_{\bar{3}}$ are the numbers of D3-branes and anti-D3-branes and where $\chi$ is the Euler character of the Calabi-Yau fourfold in F theory since the crucial negative term in the potential arises from the contribution of wrapped D7-branes which contribute negative D3-brane charge and tension of this order [2]. This latter contribution can be related to the flux background via a Chern-Simons contribution to Gauss' law [2], giving

$$\frac{1}{2g_s^2 l_s^8 T_3}\int_{M_6} H_{(3)}\wedge F_{(3)} = -Q_3^{localized} \tag{5.20}$$

where $Q_3^{localized}$ is the 3-brane charge coming from all localized sources (D3-branes, orientifold planes, and wrapped D7-branes), $T_3$ is the D3-brane tension, and $M_6$ is the base of the F-theory fourfold compactification.

For the MSS models [5], $a \sim D-10$ where $D$ is the total dimension of the supercritical theory, and $b$ comes from orientifold and antiorientifold planes and is independent of the flux quantum numbers.

In both types of models, we will take $a$ to be finite as we scale up the RR charges, and thus will include it in the "order 1" coefficients we are not keeping track of.

The parameterization (5.18) is useful because as noted in [5], $\delta = 0$ corresponds to a flat solution $\Lambda_\gamma = 0$, and for $0 < \delta < \frac{(d-2)^2}{8d}$ one finds metastable de Sitter minima with cosmological constants ranging from zero to

$$\Lambda_{\max} \sim \frac{1}{l_d^2}\frac{a^{\frac{d+2}{d-2}}8^{\frac{4}{d-2}}(d-2)^2}{b^{\frac{4}{d-2}}d(d+2)^{\frac{d+2}{d-2}}}\,. \tag{5.21}$$



JHEP12(2004)061

In this range, the dilaton does not vary much, changing from $2a/b$ to $8a/(b(d+2))$. From (5.19) and the just quoted range of $\delta_\gamma$, we see that if we just keep track of the $Q_\gamma$ dependence

$$b \sim Q_\gamma \tag{5.22}$$

in any $\Lambda \geq 0$ minimum. In particular, since $0 < \delta < \mathcal{O}(1)$ for the whole range of models, $Q_\gamma$ is of the same order for all $\gamma$ in the discrete family of models for which $b$ is independent of $\gamma$. This means that the string coupling

$$g_s \sim \frac{1}{Q_\gamma} \tag{5.23}$$

is of the same order in all of the models (in particular it does not change much as we go from one side of the D-brane domain walls to the other side). Using these relations, we see that

$$\Lambda_{\max} \sim \frac{1}{l_s^2}\,. \tag{5.24}$$

Using (5.19) for both $dS_L$ and $dS_R$, we obtain a condition on the D-brane charges required for a domain wall separating $dS_L$ and $dS_R$ if $b$ does not change in the transition:

$$\vec{Q}^2 - 2\vec{Q}\cdot\vec{Q}_L = \frac{b^2}{4a}(\delta_R - \delta_L)\,. \tag{5.25}$$

In general, this condition has many solutions depending on how $\vec{Q}$ is oriented relative to $\vec{Q}_L$. This set of solutions in general will include a range of $Q \equiv |\vec{Q}|$. This range is bounded above by $Q_R \sim Q_L$, since for $Q$ much larger than this, the condition (5.25) could not be satisfied. So for the D-brane walls in flux models, we have

$$Q \leq Q_L \sim Q_R\,. \tag{5.26}$$

(Here we are using the fact that (5.19) implies that $b$ is of the order of $Q_L \sim Q_R$ in the range of $\delta$'s we have discussed above for which dS minima exist.)

In the KKLT models, there are important other ingredients going beyond the terms so far listed in (5.18), which stabilize the volume modulus $\rho$ of $M_6$ and which also shift the minimum of the potential in the dilaton direction.

KKLT start from a no scale model [2] with complex structure moduli and dilaton stabilized by a potential which in components takes the form (5.18) in each direction in the scalar field space. This no-scale potential $\Lambda_{ns}$ satisfies $\Lambda_{ns} \geq 0$, with $\Lambda_{ns} = 0$ solutions given by setting $D_i W_0 = 0$ where $i$ runs over moduli other than $\rho$ and where $W_0$ is the classical superpotential given by [37]

$$W \sim \int_{M_6} \Omega \wedge (F_3 - \tau H_3)\,. \tag{5.27}$$

Here $\tau = C_{(0)} + i g_s^{-1}$ is the axion-dilaton and the superpotential is being evaluated at an orientifold limit of the F theory compactification where $M_6$ becomes an orientifold of a Calabi-Yau with holomorphic three-form $\Omega$.



JHEP12(2004)061

From our component expression (5.18) and the ensuing discussion, we see that

$$b = 2Q_{NS}Q_\gamma \qquad \text{for } \Lambda_{ns} = 0\,. \tag{5.28}$$

If we start from such a $\Lambda_{ns} = 0$ vacuum and change the RR flux $F$ (as we with to do using D-branes in our present application), there are two basic cases to consider. One case, appropriate to the discussion surrounding (5.25), is to consider a jump in flux for which $b$ stays constant and to take a model we obtain on the other side of the domain wall for which at the no-scale level $\Lambda_{ns} > 0$. Another possibility is to stay within the set of models given by $\Lambda_{ns} = 0$, which requires $a$ and $b$ to change appropriately to preserve (5.28). For flux jumps in which $\int H \wedge F$ changes, there must be D3-branes or anti-D3-branes ending on the D5-brane domain wall in order to preserve the relation (5.20).

In fixing the volume modulus $\rho$, KKLT employ a no-scale violating contribution to the superpotential such as a gaugino condensate to obtain an AdS minimum, and anti-D3-branes to kick the minimum up to a dS minimum. These additions roughly add

$$\Delta\Lambda \sim -e^K |W_0|^2 + T_{\bar{3}} \tag{5.29}$$

to the scalar potential, where $T_{\bar{3}}$ is the tension of the anti-D3-branes in Einstein frame, and where in the first term we have used the fact that the solution to the equation of motion for $\rho$ balances the gaugino condensate superpotential against $W_0$, leading to a negative contribution of the order of the first term in (5.29) [1]. It may be possible to eliminate the need for the anti-D3-brane contribution to $\Lambda$ by making use of $\Lambda_{ns} > 0$ metastable flux vacua in the no-scale model instead of starting from $\Lambda_{ns} = 0$ configurations and adding anti-D3-branes. We leave a detailed investigation of that for future work.

There is a rich set of flux jumps available in this set of models.[8] We will mostly confine ourselves here to verifying that the correspondence limit (5.15) we found in the model independent analysis is available in flux stabilized models.

### 5.3 Model input: correspondence point

We would like to understand whether the correspondence point (5.15) at which the D-brane entropy approaches the $dS_R$ entropy is available in the concrete flux models. This requires simply that

$$\Lambda_R - \Lambda_L \sim \Lambda_R \sim \frac{1}{l_s^2} \tag{5.30}$$

and that there exists a $Q \sim Q_L \sim Q_R$ critical bubble.

Consider now the case where $b$ does not change in the flux jumps, and where $\delta_L$ is approximately zero,[9] and $\delta_R$ is of order 1. This means $\Lambda_R$ scales like $\Lambda_{\max} \sim \frac{1}{l_s^2}$. Then to have a critical bubble, we need $T_D^2 \sim l_s^{-2} l_d^{2d-4}$ (from (5.2)), which implies $g_s \sim 1/Q$.

This is satisfied here, as we can see as follows. The condition (5.25) becomes

$$Q^2 - 2\vec{Q}\cdot\vec{Q}_L \sim \frac{b^2}{4a} \sim Q_L^2 \tag{5.31}$$

[8] See [14] for an analysis of decays arising from brane bubbles in these models.

[9] We will explain how fine the discretuum is more precisely in a future subsection.

which means that $Q$ must be of order $Q_L \sim Q_R$. So in this case we have

$$b \sim Q \sim Q_L \sim Q_R\,. \tag{5.32}$$

Then since at the dS minima $g_s \sim 1/b$, and since $b \sim Q_L$, we have from (5.32) that $g_s \sim 1/Q$.

So in this case, (5.16) is satisfied, and we are at the string scale correspondence point (5.15) where the D-brane entropy $S_D \sim Q^2$ is of the same order as the $dS_R$ entropy $S_R \sim Q_R^2$.

In the KKLT models, we can also obtain the correspondence limit in the cases where $b$ does change in the flux jumps. For example, we can consider jumps which preserve $\Lambda_{ns} = 0$ at the no-scale level, and change $W_0$ so as to adjust the negative term in (5.29). Again, it is possible to start with a nearly string scale cosmological constant and jump the flux by a $Q \sim Q_R$ D-brane bubble, which means as above that $g \sim 1/Q$ and the bubble is critical given our string-scale starting point.

We have considered critical bubbles in formulating and exhibiting our correspondence point. One might wonder about the possibility of subcritical bubbles also saturating the $dS_R$ entropy in some situation. In fact, we can rule out this possibility for $R_R \geq l_s$ from the basic feature $g_s \sim 1/Q_\gamma$ in the models. Suppose the possibility existed, which means we could start from $\Lambda_R \leq 1/l_s^2$ with a subcritical bubble saturating the $dS_R$ entropy. Then increase $Q$ to obtain a critical bubble (fixing $\Lambda_R$). Since this increases the D-branes' entropy $S_D$, it would lead to a contradiction with the result (5.14), (5.15) which show that for critical bubbles the entropy is subdominant unless $\Lambda_R$ is of order the string scale. We must check that this process of increasing $Q$ to obtain a critical bubble is possible (i.e. that $Q$ is not somehow constrained to provide only subcritical bubbles in any case). In the models, we can consider $Q$ up to of order $Q_\gamma$ as we discussed in (5.26). The upper limit $Q \sim Q_\gamma$ is not consistent with a subcritical bubble, since such a bubble would satisfy $T_D^2 < (\Lambda_R/l_d^2(d-2)$ which would imply $R_R/l_s < 1/(Q_\gamma g_s)$. But since $g_s \sim 1/Q_\gamma$, we see that this would require $R_R < l_s$ which is outside the regime of validity of the analysis. As we will see in section 6, this simple relation $g_s \sim 1/Q_\gamma$ coming from the flux models also guarantees satisfaction of Bousso's bound.

### 5.4 Model input: more generic D-Sitter spacetimes

If $\delta_R \ll 1$, we find that there exist cases with critical bubbles for which $S_D \ll S_R$, as well as a rich spectrum of sub and supercritical bubbles.

Let us begin by estimating how finely spaced the discretuum is in our situation with many fluxes, following Bousso and Polchinski [30]. If the space of fluxes is $\chi$-dimensional, then

$$\rho^2 \equiv \frac{b^2}{4a}(1+\delta_\gamma) \sim \sum_{i=1}^{\chi} q_i Q_{\gamma,i}^2 \tag{5.33}$$

where $q_i$ are coefficients we are assuming to be of order 1. This defines a $\chi-1$-sphere of radius $\rho$. Let us consider a shell between $\rho = Q_\gamma$ and $\rho = Q_\gamma + \eta$. The volume of this shell is

$$\eta \frac{\rho^{\chi-1} 2\pi^{\frac{\chi-1}{2}}}{\Gamma(\frac{\chi-1}{2})} \tag{5.34}$$

which is roughly the number of points in the shell. Setting this to one, we obtain the discretuum spacing

$$\delta_{\rm min} \sim \frac{4a}{b^2}\left(\frac{2\Gamma(\frac{\chi-1}{2})}{Q_\gamma^{\chi-2} 2\pi^{\frac{\chi-1}{2}}}\right). \tag{5.35}$$

This translates into a minimum positive cosmological constant

$$\Lambda_{\rm min} \sim \frac{1}{l_d^2} a (\frac{2a}{b})^{\frac{4}{d-2}} \delta_{\rm min} \tag{5.36}$$

with a corresponding entropy

$$S_{\Lambda_{\rm min}} \sim \frac{b^d \pi^{\frac{\chi}{4}(d-2)} Q_\gamma^{\frac{\chi}{2}(d-2)}}{\chi^{\frac{\chi}{4}(d-2)}}. \tag{5.37}$$

Now using the fact discussed in section 5.2 that for the KKLT models $b \sim Q_\gamma \sim \chi$, we obtain an estimate for the entropy in the class of examples we are considering of the form

$$S_{\Lambda_{\rm min}} \sim Q_\gamma^{\frac{\chi}{2}+4}. \tag{5.38}$$

If we consider the right dS , $dS_R$, to have cosmological constant of this scale $\Lambda_R \sim \Lambda_{\rm min}$, then the naive D-brane entropy (5.13) is very much smaller than the dS entropy because of the bound (5.26) on the flux charge we can pull out in the form of branes.

Let us make three remarks about interpreting this result. Firstly (as will also be discussed in section 5.6) in the canonical ensemble taking into account Boltzmann suppression of heavy states, in this regime far from the correspondence point, the DS entropy as seen by $\mathcal{O}_L$ is less than dS entropy, even if we include states not localized on the D-branes. Secondly, as will be discussed in section 7, the entropy associated with a putative open string theory at the horizon of the static patch in de Sitter space agrees with the entropy ascribed to the horizon of de Sitter space even in cases where it is very large as a function of flux quantum numbers as in (5.38). Thirdly, the formula (5.38) appearing here and in AdS flux models may be suggestive of a field theoretic system with many flavors.

Using the general relations in section 5.2, we can study many D-Sitter spacetimes. Let us take $\Lambda_L = \Lambda_{\rm min}$ and consider a pair of representative set of cases for $\Lambda_R < \Lambda_{\rm max}$. (The case $\Lambda_R \sim \Lambda_{\rm max}$ was studied in the previous subsection where we saw it gave rise to a correspondence point where the D-brane entropy is of the order of the $dS_R$ entropy.)

**Case I:** $(\delta_{\rm min}, \delta_{\rm min})$. First let us consider the case where $\Lambda_R \sim \Lambda_{\rm min}$, that is $\delta_R > \delta_L$ but both of order $\delta_{\rm min}$. Since $\vec{Q}_L^2$ and $\vec{Q}_R^2$ are separated by the minimal spacing $\delta_{\rm min}$, there is as we just discussed on average one lattice point in the shell between $Q_R$ and $Q_L$. This means the average separation between $\vec{Q}_R$ and $\vec{Q}_L$, namely $\vec{Q} = \vec{Q}_L - \vec{Q}_R$, has magnitude of order $Q_R \sim Q_L$. So for case I, $Q \sim Q_L \sim Q_R$.

We can compute the size of the corresponding bubble. For this case, we find that the D-brane tension $T_D$ satisfies $T_D^2 \sim Q_L^{-\frac{4}{d-2}}/l_d^{2d-2} \gg (\Lambda_R \sim \Lambda_{\rm min})$. So the bubble is highly supercritical, and $R_B \sim 0$.

**Case II:** ($\delta_{\min}, \delta_R \sim 1/Q_L$). Now let us consider an intermediate case in which $\Lambda_{\min} \ll \Lambda_R \ll \Lambda_{\max}$. If we take $\delta_R \sim 1/Q_L$, then we find (5.25) can be satisfied for a range of $Q$ from order 1 to order $Q_L$. For d=4, the former is very subcritical and the latter is supercritical; in between at $Q$ of order $Q_L^{1/2}$ we find a horizon sized bubble. Again, the D-brane entropy is generically very subdominant to the $dS_R$ entropy.

### 5.5 Constraint on the D-Sitter models from back reaction

As mentioned in section 4, we must consider the back reaction of the thermal radiation coming from the accelerating brane. If we model this as a "moving mirror" phenomenon[10] then we obtain a temperature felt by $\mathcal{O}_L$ which is of order $\rho/R_B$ where $\rho$ is the reflection coefficient for modes impinging on the brane from the "left" side; $\rho$ is $\leq 1$ and goes to zero as $\Lambda_L \to \Lambda_R$. The back reaction this produces on the curvature is of order

$$\Delta\mathcal{R} \sim G_N \left(\frac{\rho}{R_B}\right)^d \sim \left(\frac{l_s \rho}{R_B}\right)^d \frac{g_s^2}{l_s^2}. \tag{5.39}$$

In order to avoid back reaction, we must consider $\Lambda_L \geq \Delta\mathcal{R}$. This is easily achieved in the models. Note that contributions to the stress energy which simply renormalize the cosmological term can be tuned effectively with our fluxes; the values for $\Lambda_\gamma$ we quote in the analysis refer to the resulting total cosmological constant.

### 5.6 On the relation between D-Sitter and de Sitter entropy

The concrete results in this section pertain most directly to D-Sitter space. In this subsection we will explore their relation to de Sitter space itself. As we have discussed, D-Sitter space is a deformation of de Sitter space; we have compared the D-brane entropy $S_D$ probed by $\mathcal{O}_L$ at $\tau = 0$ with the entropy of the corresponding $dS_R$ space, and found it to agree up to order one coefficients in the correspondence limit (5.15). Away from the correspondence limit, the entropy localized on the D-brane bubble wall itself is parameterically smaller than that of $dS_R$ (5.14). In these cases, there is room in the D-Sitter geometry for other states (such as black holes in the middle of the bubble) but the most entropic of these states are Boltzmann suppressed in the canonical ensemble that applies at the temperature of the system.

It would be interesting to understand what the precise relation between dS and DS entropy is. In the AdS/CFT cases we discussed in section 1 and section 2, it is clear that the deformation between AdS and ADS could be made adiabatically (in the sense that one could follow the states of the system even as they mass up along the Coulomb branch); but there also if we worked in a canonical ensemble at fixed nonzero temperature the entropy would decrease as we pull branes far enough out of the horizon, since the stretched strings then become Boltzmann suppressed. In our closed cosmology it is not clear a priori whether one can deform the system adiabatically, but our result (5.15) on the string scale correspondence point exhibits a case where the deformation is adiabatic up to order one coefficients in the canonical ensemble.

[10]We thank S. Hellerman and S. Shenker for discussions on this interpretation.

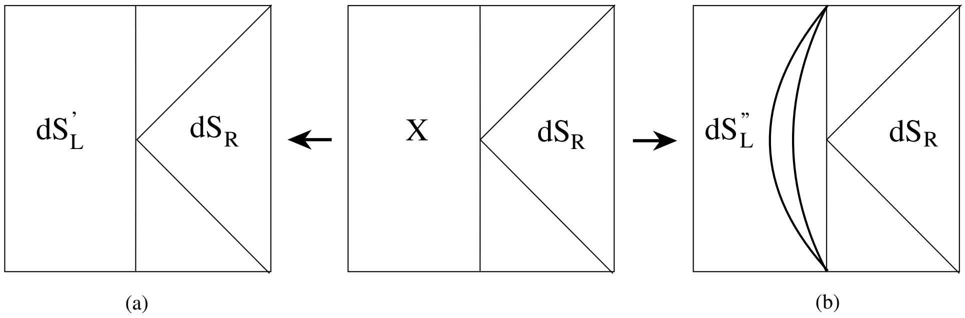


**Figure 13:** Given the geometry of the static patch of the observer on the right (at $\theta' = \pi$) to be de Sitter space $\mathrm{dS_R}$, there are still more possibilities for the global structure of the spacetime. For example, the left part of the spacetime may be $(a)$ de Sitter $\mathrm{dS'_L}$ with the same cosmological constant, or $(b)$ it may contain a domain wall and a region of a different cosmological constant.

The assertion that the de Sitter horizon area itself should correspond to an entropy [40] is based on arguments such as the following. One is the possibility of trading ordinary matter entropy for horizon area locally (see [43] for a review). Another argument based on the static causal patch in dS notes that the blueshifting of modes toward the horizon of the causal patch leads to an area's worth of high temperature modes there [15, 11, 44]; another way to view this is via the large acceleration required of an observer to probe the horizon but stay within the causal patch. (These arguments can be applied also to the time dependent causal patches such as that we found for $\mathcal{O}_L$ in section 3; one obtains different results for the entropy associated to the horizon for experiments conducted at different times.)

**Observer $\mathcal{O}_R$ and the physics behind the horizon.** One intriguing aspect of the D-Sitter geometry is the following. For the cases of subcritical or critical bubbles, the causal patch for the right observer $\mathcal{O}_R$ is the same in DS and in dS.

That is, as illustrated in figure 13, the right causal patch can be coupled consistently to the left side of D-Sitter or the left side of ordinary $dS_R$. At the perturbative level, these are distinct possibilities for the global structure of the spacetime. In other words, what is behind the horizon of $\mathcal{O}_R$ at $\tau = 0$, which in ordinary de Sitter space is the $\tau = 0$ slice of another causal patch, can be replaced by the left side of D-Sitter space. Naively one might conclude from this that the entropy of $\mathcal{O}_R$'s horizon should agree with that of the left D-Sitter space, inasmuch as this horizon entropy encodes what is behind the horizon in a given perturbative spacetime background. However, as we have discussed, the entropy of the left part of DS as measured by $\mathcal{O}_L$ in the canonical ensemble is smaller than $S_R$ away from the correspondence point.

In any case, up to order one coefficients our result (5.15) provides prima facie evidence for an adiabatic transition from string scale dS to DS.

## 6. Bousso's entropy bound

Bousso has proposed a bound on entropy going through light sheets emanating inward from any surface of area $A$ in a spacetime [20] (for a beautiful review see [43]). The covariant

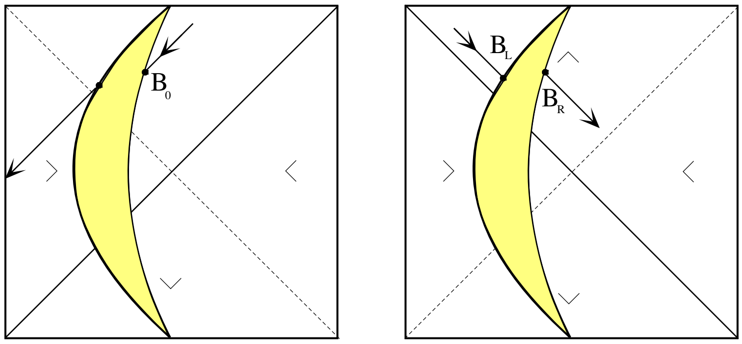


(a) (b)

**Figure 14:** Two light sheets which illustrate the covariant entropy bounds in D-Sitter space.

entropy bound is expressed in terms of light sheets, which are lightlike hypersurfaces, emanating from a chosen surface $B$ in a spacetime, which contract (or at least do not expand). The conjecture, which has been well tested in a wide variety of circumstances and proved under some assumptions [45], states that the entropy on any light sheet of a surface $B$ in a spacetime will not exceed one quarter of the area of $B$. As described in [43], the conjecture is motivated by its elegant covariance and by the desire for wide applicability of the holographic principle. Recently a refinement to take into account quantum effects has been proposed [46]. One can also formulate a related conjecture for partial light sheets [45], for which the entropy going through is bounded by the difference of the areas on the two ends. In this subsection we will analyze both of these conditions in D-Sitter space for two illustrative light sheets.

Let us examine first the statement for full light sheets. In particular, let us study what the bound predicts regarding the entropy carried by the bubbles in D-Sitter. If we pick a subcritical bubble in $dS_R$, then one can consider a spherical surface $B_0$ of area $A_0$ just to the right of the bubbles but still on the upper left quadrant of the Penrose diagram (see figure 14$a$); for such surfaces $B_0$ there exists a light sheet emanating toward the lower left in the diagram. Let us consider this light sheet for an example of a bound following from a full light sheet.

According to Bousso's conjecture, the entropy in this light sheet must not exceed $A_0/4l_d^{d-2}$. This implies that

$$S_D \sim Q^2 A_0 \mathcal{T}_B^{d-2} < \frac{A_0}{4l_d^{d-2}} \,. \tag{6.1}$$

The area drops out of this relation, which can be rewritten using $l_d^{d-2} \sim g_s^2 l_s^{d-2}$ and $\mathcal{T}_B \sim 1/R_B$ as

$$g_s^2 < \frac{1}{Q^2}\left(\frac{R_B}{l_s}\right)^{d-2} . \tag{6.2}$$

When $R_B$ is of order $l_s$, this becomes

$$g_s^2 < \frac{1}{Q^2} \tag{6.3}$$

which is satisfied for flux compactifications in string theory since (1.1)(5.23) $g_s \sim 1/Q_\gamma$ and $Q \leq Q_\gamma$. If further we are at the correspondence point $R_R \sim l_s$ for a critical bubble (5.15), then $Q \sim Q_\gamma$ so that $g_s \sim 1/Q$ and Bousso's bound is saturated for all $\tau > 0$.

Now let us illustrate the bound on partial light sheets going through the bubble wall [45] (see figure 14*b*). For example, we can work in the region where both the left and right sides of the branes are in the upper right half of the corresponding $dS_L$ and $dS_R$ Penrose diagrams. In this region, there is a light sheet with areas decreasing as one moves down and to the right on the Penrose diagram. Let us consider a slightly subcritical bubble. Let us consider a surface $B_L$ to the left of the bubble with area $A_L$, and take a partial light sheet heading down and to the right in the Penrose diagram ending at a surface $B_R$ of area $A_R$ just to the right of the D-branes, with all of the above contained in the upper left quadrant. According to the covariant entropy bound applied to this partial light sheet, we should find

$$\frac{A_L - A_R}{4 l_d^{d-2}} > S_D \,. \tag{6.4}$$

If the branes were infinitely thin, then the left hand side of (6.4) would be zero. In our case, they have a thickness (5.12) determined by their supergravity solution. Let us introduce this order of thickness in the right region of the solution (this provides the most dangerously small contribution to the change in area). The proper thickness (5.12) is also the change in $\tau$ as we go from $B_L$ to $B_R$. Using this and the relation (5.5) applicable for our almost critical bubble, we obtain

$$e^{-(d-2)\tau_R} \frac{A_L - A_R}{l_d^{d-2}} \sim \frac{L_{\text{branes}}}{l_d} \left(\frac{R_R}{l_d}\right)^{d-3} \sim \frac{(g_s Q)^{\frac{d-4}{4}} l_s}{l_d} \left(\frac{R_R}{l_d}\right)^{d-3} \sim Q^2 (g_s Q)^{-\frac{3d}{4}} \,. \tag{6.5}$$

Then the condition (6.4) becomes

$$Q^2 (g_s Q)^{-\frac{3d}{4}} > Q^2 \tag{6.6}$$

which is satisfied in our regime $g_s Q \leq 1$ (which follows from $R_R \geq l_s$ (5.8)). As before, this bound is saturated at the correspondence point. Note that in the cases $d > 4$ in which the nominal thickness (5.12) is substring scale, the condition (6.6) is stronger than we actually need to satisfy the bound since we should in that case take an effective thickness of $l_s$.

## 7. Static observers, the DS $\leftrightarrow$ dS deformation, and open strings

The left causal patch of $\mathcal{O}_L$ (figure 7) in D-Sitter and the static causal patch of $\mathcal{O}_s$ are each deformations of the causal patch of ordinary $dS_R$. As we discussed in section 2, this deformation is reminiscent of the deformation in AdS/CFT taking the field theory out along its Coulomb branch, and the causal patches of the observers $\mathcal{O}_{L,s}$ are reminiscent of the Poincare patch in AdS/CFT. This is particularly appropriate as an analogy for $\mathcal{O}_s$ for which there exists a static coordinate system covering its causal patch.

In any situation with a horizon, if there is a perturbative string description applying to a single causal patch, then since the worldsheets have boundary on the horizon there may be a dual channel open string description [11] (see also [12, 13] for other indications of an open string description of a time dependent background). A priori it is not clear how to quantize strings in such backgrounds; the nonlinear sigma model is nontrivial and the status of the S matrix is unclear. Indeed, it would be difficult to formulate the problem directly in terms of closed strings because they are in general off shell when entering or leaving the horizon.

This situation is familiar however from perturbative string theory in the presence of D-branes, which also inject off shell closed strings at some locus in spacetime. The relation to D-branes we have developed in this paper provides support for the possibility that a consistent open string theory may exist with the strings ending on the horizon. One piece of evidence was discussed in section 3 (figure 9): the observer $\mathcal{O}_s$ at a fixed distance from the brane can take a limit where the branes approach a trajectory tracking a patch of the horizon for all time; this is a limit in which the static patch for $\mathcal{O}_s$ in D-Sitter space approaches the original $dS_R$ causal patch.

Another piece of evidence arises from the success of the following simple estimate for the entropy using the relation (1.1)(5.23) in the flux models. Consider a de Sitter space with horizon area $A$ coming from a string theory compactification with flux quantum numbers $\vec{Q}_\gamma$. Assume that there is a description of the system in terms of a low energy open string theory (a field theory) with of order $Q_\gamma$ Chan-Paton factors at the horizon, corresponding to the flux quantum numbers $\vec{Q}_\gamma$. Assume further that this field theory is at a temperature $\mathcal{T}_{\rm close}$ of order the string scale (which is suggested by a picture in which the open strings end at a stretched horizon [47] corresponding to a string scale cutoff), but somewhat lower than the Hagedorn temperature such that the divergences associated with that transition do not come into play. Then the entropy is given by

$$S_{\rm close} \sim Q_\gamma^2 A \mathcal{T}_{\rm close}^{d-2} = Q_\gamma^2 A \frac{1}{l_s^{d-2}} = \frac{A}{l_d^{d-2}} g_s^2 Q_\gamma^2 \,. \tag{7.1}$$

Now using the basic relation (1.1)(5.23) $g_s \sim 1/Q_\gamma$ from the flux stabilization of the dilaton, we obtain

$$S_{\rm close} \sim \frac{A}{l_d^2} \sim S_{dS} \tag{7.2}$$

agreeing with the de Sitter entropy up to order one coefficients.

We can combine the two pieces of evidence we have gathered, and ask for a D-Sitter space with a bubble wall of $Q_\gamma$ D-branes and with $R_B$ of order string scale (realizing materially a string scale stretched horizon containing D-branes). This leads to a $dS_R$ of order string scale, putting us again at the correspondence point. However, the result (7.2) on its own seems to apply more generally.

As we mentioned in the introduction, it is important to understand how the open string theory we contemplate here (as well as the D-Sitter analysis more generally) could be extended to account for the nonperturbative decays of de Sitter models [1, 5, 14].

Finally let us note that an open string description may also apply to non-static observers such as $\mathcal{O}_L$. We have exhibited a deformation in which branes can be introduced into the left observer's causal patch; this deformation has the property that the horizon area at $T = 0$ decreases in the process (3.25), suggesting again that the branes can be thought of as being pulled out of the horizon, though in this case there is no static description and the branes do not track the horizon in the limit in which we go back to ordinary $dS_R$.

In summary, our results provide further evidence for the notion that one can describe the physics of the horizon by open strings. It is tempting to conjecture that such a description formulates quantum gravity in the causal patch for $\mathcal{O}_s$ (and maybe also $\mathcal{O}_L$); however in the cases where de Sitter decays via bubble nucleation the nonperturbative physics will not be controlled by the simple causal patch of the perturbative de Sitter solution figure 4.

## 8. Conclusions

In this paper we have studied a basic deformation of de Sitter flux compactifications — by introduction of D-brane domain walls — as an approach to the problem of exhibiting the microstates associated to flux compactifications. We have analyzed many basic properties of the resulting D-Sitter spaces. In particular, we determined the causal and thermodynamic structure of the space from the point of view of four basic classes of observers (the observer $\mathcal{O}_L$ in the middle of the bubble, the observer on the bubble wall, the observer $\mathcal{O}_s$ at a fixed distance from the wall, and the observer $\mathcal{O}_R$ outside a subcritical bubble whose causal patch is the same as that of the original de Sitter space).

We compared the entropy localized on the D-branes in D-Sitter space and measured by $\mathcal{O}_L$ to that associated with the horizon of the original de Sitter space, and found a correspondence point at which the entropies agree up to order one coefficients and at which the Bousso bound is similarly saturated for all time.

We found two pieces of circumstantial evidence going in the direction of an open string description of the de Sitter causal patch: the static observer in D-Sitter space has the D-branes approach the horizon as one takes the limit to the original de Sitter space, and the basic relation (1.1) leads to the right entropy from the low energy open string description.

As we have discussed, this work raises many interesting questions for future work. One basic question is the counting of strings stretched from the D-branes to the horizon (and in the global geometry then stretching back to a causally disconnected region of the D-brane wall). This calculation, and its analogue in ordinary AdS/CFT and in more generic AdS flux compactifications, would provide a microscopic computation of the derivative of the entropy with respect to flux quantum numbers. Another major question is the problem of further testing (and more precisely formulating) the conjecture of an open string description of $\mathcal{O}_s$'s causal patch. We plan to pursue this using the limit we discussed in which the D-branes approach the horizon. Similarly, finding a way to determine the precise relation between dS and DS entropy (perhaps by pushing further along the lines discussed in section 5.6 and section 7, or by studying black holes in D-Sitter space) is crucial for further progress. Given a clear relation between D-Sitter and de Sitter vacua, one may be able to study other aspects of de Sitter physics using the D-Sitter degrees of freedom. For example, one may be able to study the distribution and decay dynamics of flux backgrounds [30, 5, 1, 48, 49, 14] using our D-brane description, or elucidate some of the conceptual puzzles raised in e.g. [16, 17].



JHEP12(2004)061

Our approach based on the deformation of flux vacua into spacetimes containing D-brane bubbles can be applied to many more situations. For example, the Susskind-Witten entropy of AdS flux compactifications can be studied as a function of flux quantum numbers, which leads to similar questions to those discussed here regarding its interpretation in terms of D-branes. In general, any time D-brane bubbles can be extracted by deformation from a spacetime, one can study as we did here their entropy and the relation of the deformation to the original spacetime.

## Acknowledgments

We would like to thank A. Adams, T. Banks, R. Bousso, A. Frey, S. Hellerman, S. Kachru, A. Karch, A. Maloney, E. Martinec, J. McGreevy, S. Shenker, A. Strominger, L. Susskind, and C. Vafa for useful discussions. The work of E.S. is supported in part by the Israel-U.S. Binational Science Foundation. The work of M.F. and E.S. is supported by the DOE under contract DE-AC03-76SF00515, by the NSF under contract 9870115 and by the A.P. Sloan Foundation, and that of M.F. by a Stanford Graduate Fellowship.



## References

[1] S. Kachru, R. Kallosh, A. Linde and S.P. Trivedi, *de Sitter vacua in string theory*, *Phys. Rev.* **D 68** (2003) 046005 [hep-th/0301240].

[2] S.B. Giddings, S. Kachru and J. Polchinski, *Hierarchies from fluxes in string compactifications*, *Phys. Rev.* **D 66** (2002) 106006 [hep-th/0105097].

[3] A.R. Frey and J. Polchinski, $N = 3$ *warped compactifications*, *Phys. Rev.* **D 65** (2002) 126009 [hep-th/0201029].

[4] S. Kachru, M.B. Schulz and S. Trivedi, *Moduli stabilization from fluxes in a simple iib orientifold*, *J. High Energy Phys.* **10** (2003) 007 [hep-th/0201028].

[5] A. Maloney, E. Silverstein and A. Strominger, *de Sitter space in noncritical string theory*, hep-th/0205316.

[6] E. Silverstein, *AdS backgrounds from asymmetric orientifolds*, hep-th/0106209.

[7] B.S. Acharya, *A moduli fixing mechanism in M-theory*, hep-th/0212294.

[8] J.M. Maldacena, *The large-N limit of superconformal field theories and supergravity*, *Adv. Theor. Math. Phys.* **2** (1998) 231 [hep-th/9711200].

[9] L. Susskind, *Some speculations about black hole entropy in string theory*, hep-th/9309145.

[10] G.T. Horowitz and J. Polchinski, *A correspondence principle for black holes and strings*, *Phys. Rev.* **D 55** (1997) 6189 [hep-th/9612146].

[11] L. Susskind and J. Uglum, *Black hole entropy in canonical quantum gravity and superstring theory*, *Phys. Rev.* **D 50** (1994) 2700 [hep-th/9401070].

[12] A. Sen, *Tachyon matter*, *J. High Energy Phys.* **07** (2002) 065 [hep-th/0203265].

[13] M. Gutperle and A. Strominger, *Spacelike branes*, *J. High Energy Phys.* **04** (2002) 018 [hep-th/0202210].

[14] A. Frey, M. Lippert, and B. Williams, to appear.

[15] L. Dyson, J. Lindesay and L. Susskind, *Is there really a de Sitter/CFT duality*, *J. High Energy Phys.* **08** (2002) 045 [hep-th/0202163].

[16] E. Witten, *Quantum gravity in de Sitter space*, hep-th/0106109.

[17] N. Goheer, M. Kleban and L. Susskind, *The trouble with de Sitter space*, *J. High Energy Phys.* **07** (2003) 056 [hep-th/0212209].

[18] L. Susskind and E. Witten, *The holographic bound in anti-de Sitter space*, hep-th/9805114.

[19] P. Kraus, F. Larsen and S.P. Trivedi, *The coulomb branch of gauge theory from rotating branes*, *J. High Energy Phys.* **03** (1999) 003 [hep-th/9811120].

[20] R. Bousso, *A covariant entropy conjecture*, *J. High Energy Phys.* **07** (1999) 004 [hep-th/9905177].

[21] S. Hawking, J.M. Maldacena and A. Strominger, *de Sitter entropy, quantum entanglement and AdS/CFT*, *J. High Energy Phys.* **05** (2001) 001 [hep-th/0002145].

[22] J.M. Maldacena and A. Strominger, *Statistical entropy of de Sitter space*, *J. High Energy Phys.* **02** (1998) 014 [gr-qc/9801096].

[23] A. Strominger, *The dS/CFT correspondence*, *J. High Energy Phys.* **10** (2001) 034 [hep-th/0106113].

[24] T. Banks, *Cosmological breaking of supersymmetry or little lambda goes back to the future, II*, hep-th/0007146.

[25] E. Halyo, *de Sitter entropy and strings*, hep-th/0107169.

[26] V. Balasubramanian, P. Hořava and D. Minic, *Deconstructing de Sitter*, *J. High Energy Phys.* **05** (2001) 043 [hep-th/0103171].

[27] M.-I. Park, *Statistical entropy of three-dimensional Kerr-de Sitter space*, *Phys. Lett.* **B 440** (1998) 275 [hep-th/9806119].

[28] M.-I. Park, *Symmetry algebras in Chern-Simons theories with boundary: canonical approach*, *Nucl. Phys.* **B 544** (1999) 377 [hep-th/9811033].

[29] J.L. Feng, J. March-Russell, S. Sethi and F. Wilczek, *Saltatory relaxation of the cosmological constant*, *Nucl. Phys.* **B 602** (2001) 307 [hep-th/0005276].

[30] R. Bousso and J. Polchinski, *Quantization of four-form fluxes and dynamical neutralization of the cosmological constant*, *J. High Energy Phys.* **06** (2000) 006 [hep-th/0004134].

[31] S. Kachru, J. Pearson and H. Verlinde, *Brane/flux annihilation and the string dual of a non-supersymmetric field theory*, *J. High Energy Phys.* **06** (2002) 021 [hep-th/0112197].

[32] S.R. Coleman and F. De Luccia, *Gravitational effects on and of vacuum decay*, *Phys. Rev.* **D 21** (1980) 3305.

[33] J.D. Brown and C. Teitelboim, *Neutralization of the cosmological constant by membrane creation*, *Nucl. Phys.* **B 297** (1988) 787.

[34] T. Banks, *Heretics of the false vacuum: gravitational effects on and of vacuum decay, II*, hep-th/0211160.

[35] A. Karch, work in progress.



JHEP12(2004)061

[36] A. Strominger and C. Vafa, *Microscopic origin of the Bekenstein-Hawking entropy*, *Phys. Lett.* **B 379** (1996) 99 [hep-th/9601029].

[37] S. Gukov, C. Vafa and E. Witten, *CFT's from Calabi-Yau four-folds*, *Nucl. Phys.* **B 584** (2000) 69 [hep-th/9906070], erratum *ibid.* **B608** (2001) 477.

[38] B.S. Acharya and C. Vafa, *On domain walls of $N = 1$ supersymmetric Yang-Mills in four dimensions*, hep-th/0103011.

[39] S. Kachru and E. Silverstein, *4d conformal theories and strings on orbifolds*, *Phys. Rev. Lett.* **80** (1998) 4855 [hep-th/9802183].

[40] G.W. Gibbons and S.W. Hawking, *Cosmological event horizons, thermodynamics and particle creation*, *Phys. Rev.* **D 15** (1977) 2738.

[41] N.D. Birrell and P. C. Davies, *Quantum fields in curved space*, Cambridge University Press, Cambridge 1982.

[42] N. Itzhaki, J.M. Maldacena, J. Sonnenschein and S. Yankielowicz, *Supergravity and the large-$N$ limit of theories with sixteen supercharges*, *Phys. Rev.* **D 58** (1998) 046004 [hep-th/9802042].

[43] R. Bousso, *The holographic principle*, *Rev. Mod. Phys.* **74** (2002) 825 [hep-th/0203101].

[44] L. Randall, V. Sanz and M.D. Schwartz, *Entropy-area relations in field theory*, *J. High Energy Phys.* **06** (2002) 008 [hep-th/0204038].

[45] E.E. Flanagan, D. Marolf and R.M. Wald, *Proof of classical versions of the Bousso entropy bound and of the generalized second law*, *Phys. Rev.* **D 62** (2000) 084035 [hep-th/9908070].

[46] A. Strominger and D.M. Thompson, *A quantum bousso bound*, *Phys. Rev.* **D 70** (2004) 044007 [hep-th/0303067].

[47] L. Susskind, L. Thorlacius and J. Uglum, *The stretched horizon and black hole complementarity*, *Phys. Rev.* **D 48** (1993) 3743 [hep-th/9306069].

[48] L. Susskind, *The anthropic landscape of string theory*, hep-th/0302219.

[49] M.R. Douglas, *The statistics of string/M theory vacua*, *J. High Energy Phys.* **05** (2003) 046 [hep-th/0303194].

JHEP12(2004)061